Visual Field Maps in Human Cortex

Brian A. Wandell[1], Serge O. Dumoulin[1] and Alyssa A. Brewer[2]

[1]Psychology Department
Stanford University
Stanford, CA 94305-2130

[2]Department of Cognitive Sciences
University of California, Irvine
Irvine, CA 92697

Corresponding author: Brian A. Wandell, wandell@stanford.edu

Author address:

Psychology Department
Jordan Hall, Building 420
Stanford University
Stanford, CA 94305-2130
(650) 725 2466

Short title: Human Visual Field Maps

Key words: fmri, visual field maps, retinotopy, cortical magnification

Abstract

Much of visual cortex is organized into visual field maps: nearby neurons have receptive fields at nearby locations in the image. Mammalian species generally have multiple visual field maps, with each species having similar but not identical maps. The introduction of functional magnetic resonance imaging made it possible to identify visual field maps in human cortex, including several near (a) medial occipital (V1,V2,V3), (b) lateral occipital (LO-1,LO-2, hMT), (c) ventral occipital (hV4, VO-1, VO-2), (c) dorsal occipital (V3A, V3B), and (d) posterior parietal cortex (IPS-0 to IPS-4). Preliminary evidence suggests the existence of additional maps, including some in the frontal lobe. Cortical maps are arranged into small clusters in which several maps have parallel eccentricity representations, while the angular representations

alternate in visual field sign. Visual field maps have been linked to functional and perceptual properties of the visual system at various spatial scales, ranging from the level of individual maps to map clusters to dorsal-ventral streams. We survey recent measurements of human visual field maps, describe hypotheses about the function and relationships between maps, and consider methods to characterize the response properties of neurons comprising these maps.

Introduction

Modern neuroscience emphasizes the principle that human perception is determined by the properties of the brain circuitry. It is equally important to recognize that these brain circuits evolved to interpret the properties of the physical environment (Shepard, 1981; Shepard, 2001). This relationship between the physical environment and brain circuitry has been recognized by many important investigators. Newton recognized the separation of the physical stimulus and psychological interpretation – "the rays, to speak properly, are not coloured. In them there is nothing else than a certain power... to stir up a sensation of this or that colour (Newton, 1704, p. 108)." Helmholtz wrote that neural circuitry and perceptual experience are organized to estimate the physical signal: "*such objects are always imagined as being present … as would have to be there in order to produce the same impression on the nervous mechanism.* (Helmholtz, 1896, italics in original, page 2)."

The most important physical property of the visual image is its spatial arrangement. One can alter the image contrast, change colors, tilt the image, or randomly remove small regions (pixels) and still recover a great deal of essential information about the image. But if one scrambles the spatial arrangement of the image at a fine scale any realistic chance of reconstructing the original is lost. Hence, we should not be surprised to find that the spatial representation of the image features is preserved and repeated multiple times within cortex. The multiplicity of visual field representations in cortex appears to reflect an accommodation between this quintessential image property and the neural circuitry's structure. As cortex interprets different aspects of the visual image – such as its spectral composition, motion, and orientation - the cortical circuitry is organized using receptive fields that preserve the most critical image information, its spatial organization. Hence, regions of visual cortex with a variety of visual functions still preserve the visual field map.

The discovery of visual field maps. More than a century ago the ophthalmologist, Inouye, and then the neurologist, Holmes, observed strong correlations between visual field deficits and the location of the

damage within primary visual cortex (V1) (Fishman, 1997; Holmes, 1918; Inouye, 1909 ; Teuber et al., 1960). Their analysis of these correlations led to the discovery of the cortical visual field map in primary visual cortex, V1. Their measurements established several important principles including that V1 in each hemisphere encodes a hemifield and that the central fovea is represented over a larger fraction of cortical surface than a comparable extent in the peripheral visual field (cortical magnification) (Figure 1).

Insert Figure 1 about here.

Some thirty years after these neurological observations, electrophysiological mapping revealed the existence of additional visual field maps in mammalian species. In the 1940s a second map (V2) adjacent and surrounding V1 was found in both rabbit and cat (Talbot and Marshall, 1941; Talbot, 1940; Talbot, 1942 ; Thompson et al., 1950; Tusa et al., 1978), and then a third adjacent map (V3) surrounding V2 was described in cat (Hubel and Wiesel, 1965). Experiments in human showed that stimulation of primary visual cortex gave rise to a sensation at the location corresponding to the visual field map representation (Brindley and Lewin, 1968). In the 1970s investigators described additional visual field maps in monkey, including some adjacent to V1/2/3 (V4) and some located at some distance from this first posterior group (MT, now also called V5) (Allman and Kaas, 1971; Zeki, 1980). During the fifty years from 1940 to 1990, the number of visual field maps reported grew enormously and leading investigators began to hypothesize about the organization amongst the maps themselves (Felleman and Essen, 1991; Goodale and Milner, 1992; Milner and Goodale, 2006; Ungerleider and Mishkin, 1982; Van Essen and Maunsell, 1983).

Human visual field maps. In the 1980s, visual field maps were measured in intact human using positron emission tomography (PET) (Fox et al., 1987). But it was only in the early 1990s, with the introduction of fMRI (Ogawa and Lee, 1990; Ogawa et al., 1990; Ogawa et al., 1992) and novel data-analysis methods (Engel et al., 1994), that investigators could measure efficiently complete visual field maps in the intact human visual cortex (DeYoe et al., 1996; Engel et al., 1997; Sereno et al., 1995). Subsequent advances in magnetic resonance instruments, experimental methods, and data analysis algorithms produced a significant amount of new data about the organization of human visual field maps (Figure 2). The main purpose of this review is to summarize the recent visual field map measurements in human cortex.

Insert Figure 2 about here.

FMRI measurements of human visual field maps has been active because of the strong interest in the human

brain and the likelihood of clinical applications. The comparative anatomy of visual field maps provides much useful information, but there are differences between various primate species (Rosa and Tweedale, 2005) and differences between human and non-human primates (Brewer et al., 2002; Tootell et al., 1997; Van Essen, 2003) these differences make the direct measurements of human essential. A second reason for the relatively high degree of activity in human field mapping is a practical matter: it is significantly easier to use fMRI to measure visual field maps in human than to make such measurements in animal models. In part, this is because working with cooperative humans is easier than working with non-human primates. Also, MRI instruments are widely available and simpler to use than the instruments for optical imaging or single unit electrophysiology. Third, while the spatial and temporal resolution of fMRI is limited for certain neuroscience objectives (Logothetis, 2002), many visual field maps are large enough to be easily identified at the spatial resolution of fMRI.

Delineation of human visual field maps serves several goals. First, visual neuroscience theory supposes that cortical regions are specialized for specific perceptual functions. The general principle is supported by neurological cases showing that localized damage can lead to very specific visual deficits, such as achromatopsia, prosopagnosia, or akinetopsia (Zeki, 1993). That perceptual specializations are mediated by signals within maps is supported by the observation that certain maps, most notably MT, are comprised of neurons with common stimulus selectivity (direction-selectivity), these neurons are arranged in a columnar map of the a key motion parameter (direction) (Albright et al., 1984), and stimulation of the neurons in these maps specifically influences behavioral decisions about motion (Salzman et al., 1990; Salzman et al., 1992). The relationship between maps and perceptual function is not likely to be direct and unique: It is likely that more than a single map is essential for a particular visual function, and that a single map participates in multiple functions. Characterizing the responses within the maps is an essential task in understanding the cortical organization of visual functions.

Second, the visual field map organization provides a basis for quantifying the relative importance of different portions of the visual field. One important measure is the amount of cortical surface area allocated as a function of visual field eccentricity, a measure commonly called cortical magnification (Daniel and Whitteridge, 1961) (see for example Figure 1B). Some cortical visual field maps are principally devoted to processing foveal information; others less so (Dougherty et al., 2003; Engel et al., 1997; Essen et al., 1984). Quantitative measurements are also a good basis for interspecies comparisons (Van Essen, 2002; Van Essen, 2003) and a detailed analysis of the visual system pathologies (Barnes et al., 2001; Baseler et al., 2002; Baseler et al., 1999; Morland et al., 2001; Victor et al., 2000).

Third, visual field maps provide a useful way to compare or combine responses of individual observers or groups of observers. Without knowledge of the functional maps, functional responses can only be compared by identifying common anatomical landmarks. But the human brain's anatomical structure is highly varied, and methods for placing a brain within a stereotaxic coordinate system, such as Talairach (1988) or MNI space (Collins et al., 1994), rarely provide spatial certainty within half a centimeter (Di Russo et al., 2002; Iaria and Petrides, 2007; Thompson et al., 1996). Furthermore, alignment of gross anatomical features will not necessarily align cytoarchitectonic (Rademacher et al., 1993) or functional regions (Dumoulin et al., 2000). Identifying a region-of-interest (ROI) using a functional measurement, such as a map, provides much better support for the assumption that one is measuring comparable regions across individuals. There is an interesting debate about the value of ROI measurements and the optimal implementation of functional localizer scans (Friston et al., 2006; Saxe et al., 2006). This debate particularly focuses on functionally defined ROIs in visual cortex, such as fusiform face area (Kanwisher et al., 1997) and lateral occipital complex (Malach et al., 1995). However, unlike these functionally defined ROIs, the value of visual field maps for identifying common regions in different observers is acknowledged by both sides. Indeed, identification of visual field maps is a prerequisite for many neuroimaging studies of human visual cortex.

Human Mapping Methods

Visual field maps are defined with respect to the fixation point. Stimuli to the right of fixation are in the right visual field, stimuli above fixation are in the upper field, and so forth. Because the visual field shifts with the eye position but is fixed with respect to the retina, visual field maps are also called *retinotopic maps*. Neural representations of visual space with respect to a frame within the scene are called *spatiotopic* maps; there are reports that responses in visual cortex are organized with respect to a visual frame within the scene (d'Avossa et al., 2007; Goossens et al., 2006; McKyton and Zohary, 2007). These are important claims, and many labs are sure to follow-up these reports.

The maps we describe here are measured while the subject maintains fixation; in this case retinotopic and spatiotopic maps are aligned. There is no doubt, however, that the maps described here are retinotopic, not spatiotopic. It may be, however, that even responses in retinotopic maps may be influenced by eye position (DeSouza et al., 2002; McKyton and Zohary, 2007).

Visual field maps measure the stimulus location that causes the largest response in a position in cortex

(Figure 3). Many laboratories use the traveling-wave method (also called phase-encoded retinotopic mapping) with ring and wedge stimuli to measure visual field maps (Brewer et al., 2005; Dumoulin et al., 2003; Engel et al., 1997; Engel et al., 1994; Sereno et al., 1995; Wandell et al., 2005; Warnking et al., 2002). In this method, a fixating observer is presented a series of contrast patterns in concentric rings at different diameters, for example (Figure 3A). The responses to the series of rings are used to estimate the most effective eccentricity (Figure 3B). The angular measurements compare the responses to a series of contrast patterns comprising wedges that rotate around the fixation point; the responses from the different angles are interpolated to estimate the most effective angle. Taken together, the two measurements specify the most effective visual field position in polar coordinates (eccentricity, angle).

A number of experimental decisions influence the quality of the map measurements (see the discussion in (Wandell et al., 2005), page 695). When cortical locations within a map are highly responsive to a small region of the visual field, ring and wedge measurements can produce very clear maps. A modern data set measuring the response at a location within V1 to a series of rings generates a modulation that is 15-20 standard deviations above the noise (Figure 3C). These data show that within human V1 cortex responds powerfully to stimuli in a small range of visual field eccentricities. The most effective visual field location eccentricity increases smoothly measuring from posterior to anterior calcarine; this defines the eccentricity map. Similarly, there is a peaked response as the wedge changes angle, and the most effective angle varies smoothly measuring from the upper to lower lip of the calcarine sulcus (Figure 3C).

Insert Figure 3 about here.

Distinguishing visual field maps. Visual field maps can be distinguished based on a number of different features. Each map contains one full representation of the visual field. Thus, cortical locations that respond preferentially to the same visual field location cannot be in the same visual field map (Press et al., 2001). The visual field maps often border at the horizontal or vertical meridians. Consequently, early visual field mapping studies, focused on the identification of these meridians. In the traveling wave method these boundaries are associated with a reversal of the direction of the wave (phase reversal). This reversal indicates a visual field map border. These borders can either be identified manually or automatically. Manual identification incorporates all of the above criteria but lacks objectivity. Therefore automatic methods are developed which identify the borders objectively.

The first automated method computes visual field map signs (Dumoulin et al., 2003; Sereno et al., 1995). The advantage is that the method segments neighboring visual field maps without any prior assumptions about the

visual field map layout. The disadvantages, however, are that visual field maps are only distinguished if they have opposite field signs. This is not always the case. For example, V3A and LO-1 have the same field sign yielding a large undifferentiated region lateral to V3d. The visual field sign method does also not constrain how much of the visual field is represented. Another automatic method fits a model of the visual field map layout to the data (Dougherty et al., 2003). The advantage of this method is that it takes into account the full representation of the visual field maps. Furthermore, the fit allows interpolation of specific points in the visual field map which in turn facilitates measurements of visual field map properties, such as surface area and cortical magnification. The disadvantage is that the stopping criteria of this non-linear fit are less than clear cut, and it needs an a priori model of the visual field layout.

A comment on traveling-wave methods. Prior to the development of the traveling-wave method, investigators measured maps by comparing the response to a stimulus in one part of the visual field versus a blank (zero contrast stimulus) (Fox et al., 1987 ; Schneider et al., 1993; Shipp et al., 1995; Tootell et al., 1995). This procedure was repeated for several different visual field locations to define a map. The traveling-wave method provided two advantages. First, comparing a localized visual stimulus with a blank field usually creates a diffuse cortical response, spreading as much as a centimeter in V1. This response is not well-suited for spatial localization within cortex. The traveling wave method is a differential measurement that identifies the most effective stimulus from a set at each cortical location. Such differential measurements are better suited to identifying a variety of maps using neuroimaging methods (Grinvald, 1985). Second, the traveling-wave method presents stimuli of interest continually, skipping the blank field presentation. Thus, throughout the measurement one is constantly acquiring information about stimulus-driven activity rather than spending half of the measurement period obtaining control (blank) responses. This makes the method relatively efficient.

These methods are well-suited to measuring hemifield field maps with neurons that have small receptive fields, such as V1. The results we summarize in the next several sections were obtained using these methods. However, as we explain later, the traveling-wave method has limitations as well. These limitations become particularly evident when measuring maps with different properties in other locations within visual cortex. At the conclusion of this paper, we describe these limitations and some of the new developments designed to overcome these limitations.

Human Visual Field Maps

The size and location of human visual cortex. Each hemisphere of human cortex spans a surface area on

the order of 1000 cm2 (Van Essen, in press; Wandell et al., in press) and ranges between 2-4 mm in thickness (Blinkov and Glezer, 1968; Braitenberg and Schüz, 1998; Fischl and Dale, 2000). Each cubic millimeter of cortex contains roughly 50 thousand neurons (Braitenberg and Schüz, 1998), so assuming an average thickness of 2.5 mm, the two cortical hemispheres contain on the order of 25 billion neurons. Human visual cortex includes the entire occipital lobe and extends significantly into the temporal and parietal lobes (Figure 2), covering about 20% of cortex. Hence, human visual cortex contains on the order of 5 billion neurons.

Human visual field mapping initially was guided by the earlier research on monkey visual cortex and specifically macaque visual areas. The macaque data served as an excellent starting point for studies of primary visual cortex and nearby maps where there is good homology between the two species. Subsequently, the traveling-wave method (Brewer et al., 2002) and simpler methods based on responses to stimuli at the horizontal and vertical meridians (Fize et al., 2003) were performed in macaque, and these measurements confirmed the ability to identify early maps using fMRI. In recent years, as an increasing amount of visual cortex has been explored, the macaque data offer a less secure model and homologies between maps are uncertain. The comparison with non-human primate remains an important, but not limiting, source of insight for human cortical organization.

Posterior-medial maps: V1, V2, V3

Insert Figure 4 about here.

The first three human hemifield maps identified using traveling-wave fMRI measurements are located near the calcarine sulcus in the occipital lobe **(**(DeYoe et al., 1996; Engel et al., 1997; Sereno et al., 1995), Figure 4). Primary visual cortex (V1), which receives direct input from the retino-geniculate pathway, occupies calcarine cortex as a unified hemifield. Two additional maps (V2, V3) occupy a strip of cortex, roughly 1-3 cm wide, which encircles V1. V2 and V3 both contain discontinuous hemifield maps, which are divided along the horizontal meridian. This discontinuity has the effect of producing quarterfield maps in V2 and V3, each of which has one long edge representing the horizontal meridian and a second representing the vertical meridian (Horton and Hoyt, 1991).

The eccentricity representations for these three areas run together in register. The eccentricity map begins at the large foveal representation on the ventral-lateral surface near the occipital pole, and increasingly peripheral stimuli are represented at increasingly anterior positions along the medial surface, forming a

semicircular pattern. In addition to the parallel eccentricity map, the vertical meridian representations of V1/V2 are adjacent to one another as are the horizontal meridian representations of V2/V3.

The pseudo-color map of eccentricity shows clearly that more cortical surface area is allocated to the central than peripheral representation (cortical magnification). The eccentricity map is reasonably well described by a simple exponential form described in several papers. Initial reports suggested that the human central representation was expanded compared to macaque (Sereno et al., 1995). However, subsequent measurements using similar methodologies in both species demonstrated that the cortical magnification in human and macaque are quite similar (Brewer et al., 2002; Engel et al., 1997).

Apart from the overall scale, the angular and eccentricity maps in these three maps are quite similar in human and macaque. Common features include the large confluent foveal representation, the concentric, unified organization of the eccentricity maps across the three areas, and the separation of the V2 and V3 maps into quarterfield representations surrounding V1. Some confusing nomenclature still arises in the literature regarding V3. In macaque, Van Essen and colleagues initially observed anatomical differences between the dorsal and ventral quarterfield representations surrounding V2 and proposed dividing V3 into two distinct areas. They named the dorsal map V3 and the ventral map VP (Burkhalter et al., 1986). This nomenclature is occasionally used to identify the dorsal and ventral strips of human V3. However, human fMRI measurements of visual field maps and function support combining the dorsal and ventral maps into one map; hence, the human maps in these positions are most commonly called V3-dorsal and V3-ventral (V3d & V3v). Recent anatomical measurements in macaque suggest that in fact the connectivity is in fact similar between macaque V3 and VP. This further supports the idea that these two quarterfield maps are part of a single functional entity (Lyon and Kaas, 2002; Wandell et al., 2005; Zeki, 2003).

Dorsal maps: V3A, V3B, and IPS-X

Insert Figure 5 about here.

Several research groups confirm the existence of a collection of visual field maps in dorsal cortex, extending from the anterior portion of V3 into the intra-parietal sulcus (IPS) (Figure 5). The map directly adjacent to V3 has many similarities to macaque V3A and is given the same name. A map sharing a confluent fovea with V3A, and now called V3B, was also observed by many groups. More recently, several smaller (400-700 mm^2) maps have been identified on the posterior portion of the intraparietal sulcus and forward several

centimeters (Press et al., 2001; Schluppeck et al., 2005; Sereno et al., 2001; Silver et al., 2005; Tootell et al., 1998). The organization of the human visual field maps beyond V3 and V3A may diverge from the macaque maps, and thus we follow a neutral labeling scheme from the human literature, in which the maps in the IPS are numbered according to their position (Swisher et al., 2007; Wandell et al., 2005).

V3A and V3B. Adjacent to the dorsal quarter-field of V3 (V3d), human cortex contains a hemifield map. The human map borders the anterior portion of V3d and was described in the early human fMRI cortical mapping papers as an angular representation beyond V3 near the transverse occipital sulcus (TOS) (DeYoe et al., 1996; Tootell et al., 1997). This region was called human V3A, because its location is similar to macaque V3A. As in macaque, human V3A represents a full hemifield. The angular representation begins at the lower vertical meridian at the border with V3d, spans the horizontal meridian and then continues into the upper visual field to end at the upper vertical meridian. Notably, V3A only borders V3d in the anterior region that represents the peripheral visual field.

Dorsal and lateral to V3A there is another hemifield map, V3B. The V3A and V3B maps share a discrete fovea located in the posterior portion of the intraparietal sulcus (IPS). This foveal representation is separate and anterior to the confluent fovea of V1/2/3 (Figure 5). Similar to the V1/V2/V3 maps, the angular representations of V3A and V3B partition the confluent eccentricity representation into two discrete maps. The eccentricity map near the foveal representation in the posterior intraparietal sulcus represents increasingly peripheral locations in the visual field in both lateral and medial directions. The corresponding angular maps of V3A and V3B span both the lateral and medial eccentricity representations: the relatively medial map is V3A, while the relatively lateral map is V3B.

There is now a consensus that the V3B map exists. Unfortunately, some of the early descriptions in the literature - including from this lab - were confusing or inaccurate. These errors have now been corrected in recent papers (Larsson and Heeger, 2006; Swisher et al., 2007) and we repeat the correction here. Smith et al. first described a map they called V3B (Smith et al., 1998). This map was adjacent to the central representation of dorsal V3. This map can be seen in Press et al. (2001, Figure 3), but those authors incorrectly labeled a different map, sharing a foveal representation with V3A, as V3B. In fact, the map they called V3B was a new map and not the original map proposed by Smith. The confusion likely arose from differences in the clarity of the eccentricity measurements near V3A between different labs; Press et al. found a very clear, discrete foveal representation for V3A that had been harder to resolve in the earlier measurements of Smith and others. Over time, the V3B label stuck with the map adjacent to V3A. Some number of years later, Larsson and Heeger (Larsson and Heeger, 2006) rediscovered the original map

identified by Smith et al., located on the lateral occipital surface, as well as another adjacent to it.

Larsson and Heeger proposed that we retain the V3B name for the map that shares a confluent fovea with V3A, and that we introduce new labels for the two more lateral maps; the one originally described by Smith is called LO-1 (lateral occipital -1), and the new map inferior and adjacent to LO-1 is called LO-2. Swisher et al. (Swisher et al., 2007) followed this notation. We agree and use that terminology here.

IPS-0 (V7). Tootell *et al*. (1998) described a map located immediately anterior to V3A that they named V7. This map begins with a representation of the upper vertical meridian at the border of V3A, spans at least a hemifield of visual space (Press et al., 2001), and contains a second dorsal foveal representation distinct from that of V3A/V3B. This region may be in the same location as macaque area DP, but there is no evidence yet for a homology between these regions. Measurements of spatial attention by Tootell *et al.* (1998) showed an increase in MR signal within V7 when attention was directed to the same retinotopic location as a visual stimulus. V7 lies within the IPS and shares a confluent fovea with another hemifield map along the IPS, IPS-1, suggesting that the two maps form a cluster. Therefore Swisher *et al.* (2007) proposed renaming V7 as IPS-0. We follow the IPS-0 nomenclature because it better describes the anatomical position of this visual field map.

IPS-1/2/3/4. Several maps along the intra-parietal sulcus (IPS), anterior to IPS-0, have been described. Sereno et al. (2001) identified a map many centimeters anterior to IPS-0, using an eye-movement memory task. They write that "unlikely that our large parietal activations were due to passive sensory responses (p. 1352)", and they speculate that this map is a homologue of macaque lateral intraparietal area (LIP). Using a variety of techniques, including eye movements and attentional modulations, Silver et al. (2005) and Schluppeck (2005) identified two visual field maps anterior to IPS-0. The first of these, IPS-1, shares a confluent fovea with IPS-0 and appears to form a cluster (Swisher et al., 2007). The second, IPS-2, can be identified from a reversal in the angle map and is further anterior. They show that IPS-1 and IPS-2 can be identified both using saccades and with attention shifts. Schluppeck et al. (2005, p. 1381) point out that these maps are posterior to the map reported by Sereno et al. (2001) using the delayed-saccade task.

Swisher et al. (2007) confirmed the location and properties of the IPS-1/2 maps in detail. In addition, they showed that these maps could be identified using sensory stimulation, without a saccadic or attentional manipulation. Moreover, they describe two visual field maps anterior to IPS-2, which they labeled IPS-3 and IPS-4. It is possible that IPS-3 corresponds to the map identified by Sereno et al. (2001).

Jack et al. (2007) report measurements of retinotopy with the goal of resolving some apparent differences between the some of the other investigators; for example, Sereno et al. (2001) did not find IPS-1 or IPS-2. The experimental paradigm used by Jack et al. uses an eye-movement and an odd-ball task to detect retinotopy, and this group does not find the IPS maps. This contrasts with Swisher et al. who used powerful statistical methods and high contrast stimuli. We note that there are many ways to fail to find a map, consequently multiple reports of the same pattern from different labs should not be outweighed by the inability to see these maps using different paradigms (see discussion in (Wandell et al., 2005)). Finally, the question of the relationship between these reported human maps, LIP in macaque, and limits to topography are discussed extensively in these papers. There is no consensus.

Lateral maps: LO-1, LO-2, hMT

Insert Figure 6 about here.

LO-1, LO-2. Responses to traveling-wave stimuli in lateral occipital (LO) cortex, a region extending lateral and anterior from dorsal V3, differ substantially from responses in primary visual cortex. We attribute this to a difference in receptive field size between neurons in V1 and LO cortex (Dumoulin and Wandell, in press). Conventional traveling-wave methods are not well-suited to uncovering visual field maps under these conditions, and several early measurements using the traveling-wave method reported confusing results and no compelling retinotopy (Tootell and Hadjikhani, 2001).

Recent compelling reports identify two clear hemifield maps, adjacent to the central representation of V3 on the lateral occipital surface (Larsson and Heeger, 2006; Press et al., 2001, Fig 3; Smith et al., 1998; Swisher et al., 2007) (Figure 6 and see also Figure 5). These maps represent the contralateral visual hemifield; they have a foveal representation that is confluent with that of V1, V2, V3 and hV4. The angle representation in LO-1 is the mirror of V3, and that in LO-2 is the mirror of LO-1. In both cases, the representation at the boundary is at the upper (V3/LO-1) or lower (LO-1/LO-2) vertical meridian. The visual field eccentricity in LO-1 and LO-2 are parallel. Currently, it is not clear whether there is a gap between the relatively anterior map (LO-2) and hMT.

The naming conventions associated with LO cortex are confusing. Investigators measuring object and face recognition observed modulations that span lateral occipital and ventral occipital-temporal cortex. They named the entire functionally-defined zone as the lateral occipital complex (LOC) (Grill-Spector and Malach, 2004; Malach et al., 1995). Tootell et al. (Tootell and Hadjikhani, 2001) subsequently described some

puzzling retinotopic responses and proposed dividing LO into two regions representing the central (LOc) and peripheral (LOp) visual field. They also use the term V4d-topo to describe parts of this region.

The notation LO-X seems appropriate for visual field maps in lateral occipital cortex and is consistent with the nomenclature for the ventral (VO-X) and dorsal (IPS-X) maps (Larsson and Heeger, 2006; Swisher et al., 2007; Wandell et al., 2005, p. 700). Based on retinotopic responses seen in our data and that from other labs, we suspect that over time the entire LOC and other regions on the ventral and lateral surface will be subdivided into visual field maps. Should this occur, the LO Complex will be divided into maps identified as either LO-X or VO-X, according to their anatomical location.

hMT+. The human homologue of macaque MT (also referred to as V5) is found within a highly motion-sensitive region on the border between lateral occipital and temporal cortex (Dumoulin et al., 2000; Tootell et al., 1995; Watson et al., 1993). The functional definition of this region probably includes several visual field maps in addition to hMT (e.g. MST). To acknowledge the imprecision in the identification, the region defined by motion responsivity is referred to as hMT+ or the V5-complex.

The initial definition of MT in monkey was based on a visual field map (Allman and Kaas, 1971). Hence, there is a strong presumption that one should be able to identify a specific human MT map. Several attempts have been made to subdivide the region hMT+ using visual field maps and other functional measurements. There is a particular focus on separating hMT from an adjacent area identified in monkey, MST (Beauchamp et al., 2007; Dukelow et al., 2001; Goossens et al., 2006; Huk et al., 2002; Smith et al., 2006). Huk et al. (Huk et al., 2002) reported the existence of a visual field map within the region hMT+, and they proposed that this visual field map is hMT. The small size of the MT visual field map and the highly folded nature of the cortex make this region difficult to study. While the presence of at least one visual field map is certain, multiple small maps are likely to exist in this region. The literature contains several images that show suggestive maps in the hMT+ region, and we suspect that with improvements in technology the maps will clarify in the next several years.

Ventral Visual Cortex: hV4, VO-1, VO-2

The organization of visual cortex beyond ventral V3 (V3v) was controversial for several years (Hadjikhani et al., 1998; Levy et al., ; McKeefry and Zeki, 1997; Wade et al., 2002; Zeki et al., 1998; Zeki et al., 1991). As fMRI measurements have become more refined, the clarity of the organization of ventral maps has improved (Figure 7).

Insert Figure 7 about here.

hV4. Directly abutting the ventral portion of V3 is a hemifield map which shares a common eccentricity orientation with the confluent foveal representation of V1/V2/V3 (Figure 7 and see also Figure 6)(Brewer et al., 2005). We refer to this map as hV4 because part of this map has already been named V4(v) by other investigators. The difference between the human hV4 map and the macaque V4 map appears substantial (Brewer et al., 2005; Brewer et al., 2002), and the homology between hV4 and macaque V4 remains unproved. Therefore, we add the 'h' to clarify that this map may not be homologous to V4 in other species. The hV4 eccentricity representation parallels that of V1/V2/V3, although the map may differ quantitatively (Ejima et al., 2003). At this point in time, many authors have used reported measurements consistent with the hV4 map that is more than a quarterfield adjacent to ventral V3 (Brewer et al., 2005; Gardner et al., 2005; Larsson and Heeger, 2006; Merabet et al., 2007; Montaser-Kouhsari et al., 2007; Swisher et al., 2007; Wade et al., 2002), and we believe there is substantial evidence for this representation.

VO-1, VO-2. Beyond hV4, there are at least two hemifield maps, VO-1 and VO-2. The lower vertical meridian representation of the VO-1 map abuts the peripheral representation of hV4 and extends to the peripheral representation of V3v. VO-1 and VO-2 share an upper vertical meridian representation. The VO-1 and VO-2 eccentricity maps begin in a large distinct foveal representation. Much like the V3A/V3B maps, the eccentricity representation forms a semicircular pattern. The eccentricity map becomes increasingly peripheral as it extends medially across the collateral sulcus and approaches the peripheral representation of V3v. We note that the definitions of hV4 and VO leave no room for the map originally labeled as V8. The difference between the hV4 and V8 model is mainly with respect to the field map organization; many features of the data described in the original V8 paper, particularly the displaced foveal representation, have been described consistently (Brewer et al., 2005; Hadjikhani et al., 1998). However, with the refinement of visual field mapping measurement methods, several labs have now shown that the specific details of the map organization in this region do not support the original V8 definition (Brewer et al., 2005; Larsson and Heeger, 2006; Swisher et al., 2007; Wade et al., 2002).

Like V1, the surface area of each of these maps varies across subjects (Dougherty et al., 2005). Increasing the stimulus radius from 3 to 16 degrees expands the responding surface area of V1 considerably along the calcarine sulcus, but the hV4, VO-1 and VO-2 maps expanded very little or not at all. These ventral maps appear to respond more powerfully to central visual stimuli throughout their extent, consistent with the strong cortical magnification described in human and macaque ventral cortex (Baizer et al., 1991; Ejima et al., 2003).

Anterior to the VO cluster, our lab has observed traveling-wave responses in many subjects (Brewer et al., 2005; Wade et al., 2002). These measurements have not yet been organized into definitive maps. Nevertheless we have identified another foveal representation, (Wandell et al., 2006) and we suspect that this foveal representation indicates the presence of another visual field map cluster. We propose to term this putative cluster ventral-temporal (VT), with corresponding visual field maps termed VT-1 and so forth.

Pre-frontal and V6 Field Maps

Two groups reported a new human visual field map they labeled V6 (Pitzalis et al., 2006; Stenbacka and Vanni, 2007). This map is identified as having a large peripheral representation, so that it is only revealed by measurements with very wide field stimuli. The map is located in the parietal-occipital sulcus, anterior to V3d. The reported absolute position and the map properties appear variable in the published figures. Much of the support for the existence and naming of the human map is based on arguments concerning the homology with the V6 map identified in macaque (Galletti et al., 1996; Galletti et al., 1999).

Two groups report topographically organized responses in frontal cortex (Hagler et al., 2007; Hagler and Sereno, 2006; Kastner et al., 2007). Although these regions are driven less by stimulus contrast than memory-guided spatial representations, the principal of topography extends beyond sensory maps to related cognitive representations of space.

The Organization of Visual Field Maps

There is significant variability in the size and position of many of these visual field maps between subjects. There have been several efforts to quantify the variation in size of primary visual cortex, specifically, and all groups agree that the surface area of V1 commonly varies by a factor as large as 2.5 even among individuals with normal visual function (Amunts et al., 2000; Dougherty et al., 2003; Stensaas et al., 1974). Despite these variations, there is much regularity in the position and properties of these maps. In a series of papers, Van Essen and his colleagues have worked to create an atlas that summarizes the key features (Van Essen, 2005). The continuing advances in discovering new maps make the accumulation of this information a daunting task. That summary is an ongoing project that contains valuable both for scientists seeking to understand the visual pathways and clinicians looking for general guidance about organization and function.

In addition to a summary of the data, several authors have tried to develop hypotheses describing the overall functional and structural organization visual field maps. These ideas are not enormously precise, nor are they

mutually exclusive. We think that efforts to understand the organization of visual cortex and these maps are important, and so we review several suggestions here.

Insert Figure 8 about here: A Ungerleider B Felleman.

Two hypotheses about the organization of visual field maps have been particularly influential (Figure 8A). Ungerleider and Mishkin (1982) noted that projections from V1 are carried via two major white matter pathways towards ventral and dorsal extrastriate cortex. They further marshaled evidence showing that ventral occipitotemporal lesions produce visual discrimination deficits, while dorsal occipitoparietal lesions produce spatial deficits, as in a landmark task without degrading object discrimination. Ungerleider and Mishkin (1982, p. 549) hypothesized that the ventral pathway is specialized for 'identifying *what* an object is" and the dorsal pathway is specialized for "locating *where* an object is" (Figure 8A). The ventral and dorsal pathways are dominated by central and peripheral signals, respectively (Baizer et al., 1991). Milner and Goodale (Goodale and Milner, 1992; Milner and Goodale, 2006) supported the concept of two major functional subdivisions of visual cortex, but they reinterpreted the data and suggested that the streams have different functional objectives. A rough summary of their view is that the ventral stream represents vision for perception, while the dorsal stream represents vision in service of action.

The principle that the visual pathways comprise two (or more) functional systems is an important part of visual neuroscience theory. The Duplex theory of rod and cone vision is perhaps the best known example; the multiple pathway hypotheses based on a multiplicity of retinal outputs with distinct central targets is yet another important example (Schneider, 1969; Trevarthen, 1968; Wandell, 1995). The idea that cortical maps represent individual functional specializations (Zeki, 1990) or that groups of maps are organized to perform specialized functions, is a natural extension of this basic neuroscience principle.

A second important organization was developed by Van Essen and colleagues (Figure 8B). They introduced an anatomical method for developing a hierarchical graph that captures the relationship between visual areas (Felleman and Essen, 1991; Van Essen and Maunsell, 1983). The relationships between visual areas were summarized in a table that classified the connections between areas as ascending, lateral, and descending. The classification was based on the laminar distribution of the connections between areas. They showed how the classification of the connections could be organized into a hierarchical graph beginning in 'lower tier' areas, including the LGN and V1, and continuing to 'higher tier' such as TEO (Figure 8B). The same data set was analyzed by Young (1992) who used multi-dimensional scaling to create a non-hierarchical visualization of these data.

Van Essen and colleagues built the hierarchical model as a working summary that could be changed as additional information was accumulated; they were aware that their very large data set contained some substantial uncertainties. There are a number of new developments, such as much new knowledge about the significance of the laminar distribution of projections (Barbas and Rempel-Clower, 1997; Pandya et al., 1988) and the identification of pathways from the LGN to V5 (Bourne and Rosa, 2003; Sincich et al., 2004) that might be incorporated. Also, the question of how sub-cortical areas fit within the hierarchy, including the whole of the thalamus, is important and under active exploration (Sherman and Guillery, 2001).

Finally, we note two recent proposals about the organization of human visual field maps. Malach and colleagues (Hasson et al., 2003; Hasson et al., 2002; Levy et al., 2001) describe ‘a new organizing principle in which object representations are arranged according to a central versus peripheral visual field bias’ (Levy et al., 2001). They suggest that after the precise lower-tier visual field maps (V1, V2 and V3) is replaced by much cruder, or absent, maps that are organized around representations of perceptual entities, including faces, places, and objects. They suggest that major features, such as the angle representation, are absent; the maps retain only an eccentricity bias that is influenced by the retinal image size of the object represented by the area. This "Eccentricity-bias" model is reviewed in (Grill-Spector and Malach, 2004, p. 668 et seq. and fig. 12).

Improvements in the measurements have revealed more visual field maps in lateral occipital cortex than Malach and colleagues anticipated when framing their hypothesis. In view of these developments, Wandell et al. (Wandell et al., 2005, p. 701) suggested an alternative organization (Fig. 9). Specifically, they propose that maps are organized into several clusters. A cluster is a group of maps with parallel eccentricity representations; different clusters have distinct eccentricity maps. Within a cluster, the maps can be identified by reversals in the visual field map angle representation. The maps near V1 are the prototypical cluster, but several other clusters - such as near V3AB, IPS, hMT+ and VO - have also been identified (Swisher et al., 2007; Wandell et al., 2006).

Insert Figure 9 about here.

Improving Visual Field Map Measurements

The traveling-wave methods successfully identified many visual field maps, but the methods have significant limitations (see earlier discussion). In the last several years new methods have emerged that may improve the ability to measure the visual field maps in visual cortex. These methods also promise to identify

additional information about the neurons within the map.

Consider some of the limitations with the traveling-wave method based on conventional ring and wedge stimuli. This method and stimuli are poorly designed for measuring maps containing neurons with receptive fields spanning the central visual field representation (Dumoulin and Wandell, in press; Press et al., 2001, Figure 7). This deficiency can be seen in two ways. First, a neuron with a receptive field centered on the fixation will not respond; neurons with slightly displaced receptive field centers will only respond slightly. This limitation is crucial because the fovea is probably the most important component of the perceptual representation. Similarly, traveling-wave estimates of the eccentricity map using expanding rings are distorted, again most prominently when cortical response regions overlap with the fovea (Dumoulin and Wandell, in press).

Second, because conventional ring and wedge stimuli do not include any blank (control) stimuli, they fail to discriminate between conditions in which the stimulus effectively drives a cortical response at a constant level from conditions in which the stimulus fails to drive a cortical response at all. Continuing with the example of a receptive field centered on the fovea, a rotating wedge stimulus drives a response at all angles - but there is no modulation. The conventional traveling-wave method - or even a method that contrasts horizontal and vertical meridians - treats this as non-responsive cortex. To detect the fact that cortex responds to all orientations, it is necessary to include a blank control. These examples illustrate that the traveling wave method and conventional wedge and ring stimuli are poorly designed for reconstructing visual field maps that contain neurons whose response region overlaps with the fovea. In V1/2/3, it is difficult to obtain high quality maps in the representations of the central 0.5-2 degrees; in parts of cortex in which receptive fields are larger, the poor measurement range spans an even larger part of the visual field.

Alternative stimulus sequence. Several groups proposed using temporally orthogonal stimulus sets to measure visual field maps (Buracas and Boynton, 2002; Hansen et al., 2004). For example, Vanni et al. (2005) proposed an interesting approach to overcoming these problems by restructuring the stimulus. Rather than systematically sweeping out the eccentricity or angle, they create a series of patches derived from the rings and wedges. These images are constructed in such a way that each of the patches has its own, unique temporal sequence. The construction of these stimulus sequences are commonly used in multifocal EEG/MEG measurements, and there are a variety of ways of constructing the orthogonal sequences. One approach is use the M-sequence method developed by Sutter, *et al*(1992). They use a general linear model (GLM) to derive how effectively each stimulus patch contributes to the response at each cortical location. They show that within V1 the simple linear model approach accurately identifies the visual field position that

most effectively stimulates each cortical location; this produces a visual field map.

This method has several advantages. First, it includes a blank stimulus, making it possible to assess whether all the stimuli are equally effective. Second, the method avoids the difficulties rings and wedges have when neuronal receptive fields span the fovea because the stimuli comprise spatially localized patches. Third, the method allows a description of the population receptive field (Yoshor et al., 2007). The method depends significantly on the assumption that the BOLD response is linear across space (see e.g., Engel et al. (1997), who made this assumption when measuring the spatial resolution of the BOLD signal). While spatial linearity was not specifically tested until the work by Hansen et al. (2004), it appears to be a good approximation for signals in V1. Whether spatial linearity is satisfied in other extrastriate regions remains to be tested. At present, however, there are no regions where M-sequences uncover maps that are missed by conventional traveling-wave methods. The advantages remain to be demonstrated.

Model-based analysis of the time-series. As the alternative name (phase-encoded retinotopic mapping) for the traveling-wave method implies, the method does not interpret all the information in the time-series response. Rather, the method uses the phase of the time-series modulation to find the most effective visual field position. From the earliest papers, however, investigators were aware that the time-series contains additional information. For example, Tootell et al. (1997) noticed that V1 and V3A time-series responses to the same stimulus differed; they interpreted these as reflecting differences in the receptive field size of neurons in these maps. Other investigators used additional measures of the time-series (duty cycle) to identify differences between neural populations in different maps or between portions of the maps representing the central and peripheral visual field (Larsson et al., 2006; Li et al., 2007; Smith et al., 2001).

Thirion et al. (2006) developed an analysis designed to use the full time-series information to decode the visual stimulus in the occipital lobe. The stimulus reconstruction was performed using two different algorithms, one based upon explicit forward model based upon the traveling wave paradigm and a second implicit reconstruction based on data classification techniques. Both algorithms predicted the stimulus with significant accuracy. However, the implicit data-classification techniques performed better, which Thirion et al attributed to shortcomings of the time-series analysis by the traveling wave method.

Insert Figure 10 about here.

The trend towards using more time series information is continuing. Dumoulin and Wandell recently developed methods for using the fMRI time series to model neuronal populations (Figure 10)(Dumoulin and Wandell, in press). Specifically, they compute a model of the population receptive field (pRF) from

responses to a wide range of stimuli and estimates the visual field map as well as other neuronal population properties, such as receptive field size and laterality. This method decouples the field map measurements from the rings and wedges, thus eliminating some of the difficulties with the conventional traveling-wave approach. They show that visual field maps obtained with the pRF method are more accurate than those obtained using conventional visual field mapping, and they trace the visual field maps to the center of the foveal representation. The pRF method promises to generalize the previous visual field mapping methods at the cost of a high computational demand.

Conclusions

During the past fifteen years functional MRI has produced a wealth of data about human visual field maps. We are not at the end of the process: improvements in MR instrumentation, as well as new analytical methods, promise to yield more insight into these functional structures. Further, new advances in MR and computational methods, such as diffusion-weighted imaging coupled with tractography, MR-spectroscopy, and MR-relaxometry, will provide more precise information about the molecular and cellular organization of visual cortex. These advances are certain to provide important tools for answering questions about human visual functions, including development, plasticity, and perceptual function.

Figure Captions

Figure 1. Human visual cortex and V1 visual field map. (A) Human visual cortex (*orange overlay*) occupies approximately 20% of the cerebral cortex and is located in the occipital lobe and posterior parts of the parietal and temporal lobes. Primary visual cortex (V1) is located in and around the calcarine sulcus (dotted line) and contains a map of the visual field. (B) We illustrate the visual field map in V1. The image is a section of Godfrey Kneller's 1989 portrait of Sir Isaac Newton. The figure illustrates how the visual field (left) is transformed and represented on the V1 cortical surface (right) using a mathematical description proposed by Schwartz (Schwartz, 1977). The left visual field stimulates V1 in the right hemisphere; the image representation is inverted, and the center of the visual field, near the eye, is greatly expanded (cortical magnification).

Figure 2. Visual field maps in human visual cortex. The most prominent maps are shown on an inflated rendering of the cortical surface. Fovea and upper/lower visual fields are indicated by the ‘o’, ‘+’, and ‘-’ symbols, respectively. The posterior visual maps in and around calcarine are labeled V for visual and a number, e.g. V1, V2, V3, V3A, following the naming of homologues in macaque monkey. Because of doubts

about the homology of the fourth visual map between monkey and human caused this map is named hV4. Because of difficulties in measuring the single map (hMT) the region in motion-selective cortex is typically labeled hMT+. Maps in lateral occipital are numbered as LO-x, maps in ventral occipital are numbered as in VO-x; maps in the intraparietal sulcus are numbered IPS-x. The homology to macaque in these regions is unclear.

Figure 3. Traveling wave-method. Traveling-wave stimuli comprise a set of contrast patterns at different eccentricities or angles. We show an example of one stimulus frame from the expanding ring (A) and rotating wedge (B) stimulus sequence. The arrows indicate the direction in which the contrast pattern sections are moving in sequential stimulus frames, but are not present in the stimulus. The fMRI responses elicited by these stimuli produce a modulation on the order of 1-3% of the BOLD signal (C). This modulation is on the order of 20 standard deviations above the background noise. The time (phase) of the peak modulation varies smoothly across space. In our example, space represents distance along the calcarine sulcus (indicated by the dashed lines in panels E and F). The time delay (phase) is used to define the most effective stimulus location for the ring (eccentricity) and wedge (angle) stimulus sequence. The inflated cortical surface (D) near calcarine (E and F) is overlaid with a color map showing the response phase at each location for an eccentricity (E) and angle experiment (F) (see the colored legends). The data show that calcarine includes a hemifield map of the contralateral visual field: V1. Only locations near the calcarine sulcus are colored, and only locations with a powerful response are shown.

Figure 4. V1, V2 and V3 visual field maps. Angle maps were measured using rotating wedges and eccentricity maps were measured using expanding rings on the same brain. The color overlay indicates the visual field angle (right) or eccentricity (left) that produces the most powerful response at each cortical location. The stimuli covered the central 20 degrees of eccentricity. For clarity, only responses near the medial occipital cortex are shown. The stimulus-driven responses shown in this paper are substantially above statistical threshold ($p < 0.001$, uncorrected). Other details as in Figure 3.

Figure 5. Visual field maps on the dorsal and lateral surface of the human brain. Angular mapping with a rotating wedge stimulus produces modulation of the BOLD signal in a substantial portion of posterior cerebral cortex (see also Wandell (2005, Figs 7 & 8)). The images shown here are reprinted from Swisher et al. (2007), and they show the right hemisphere of a single subject. (A) The reconstructed pial surface is shown from posterior lateral (top left), posterior medial (bottom left), and posterior (right) views. In these views, the cortex is folded as in the normal anatomical state. (B,C) The value of inflation for visualization is illustrated; notice that the data within the sulci that are occluded in the previous images become visible, and it is much easier to appreciate the reversals in the angular representation that are an important indicator of the

boundary between visual field maps (solid and dashed lines).

Figure 6. Visual field maps illustrated on a computationally flattened cortical representation (after Larsson and Heeger, 2006, Fig 1). A flattened representation of cortex illustrates the spatial relationship between maps near the occipital pole in the right hemisphere. The maps show the angular (left) and eccentricity (right) maps averaged across 15 hemispheres. In the left column, color indicates polar angle (inset legend). In the right column, color indicates eccentricity between 0 and 6° (inset legend).

Figure 7. Visual field maps on the ventral occipital-temporal surface of the human brain. Eccentricity and angular measurements illustrating ventral occipital maps. The left hemisphere ventral occipital region of interest is shown in the center inset. Eccentricity (right) and angle (left) measurements using a 3 degree expanding ring stimulus. White lines indicate the estimated boundaries between several visual field maps, including the ventral portions of V1, V2 and V3 as well as hV4 and VO-1 and VO-2. For clarity, only responses within these visual areas are colored, and only locations with a powerful response are shown. Other details as in Figure 3.

Figure 8. Theories of visual field map organization. (A) Signals in V1 and nearby maps are essential for conscious vision; damage to these maps causes a visual blindspot (scotoma). Signals that emerge from these maps and enter two large white matter tracts (the superior and inferior longitudinal fasciculus) are specialized for distinct visual functions. Damage in the projection zones of these tracts does not cause complete blindness but rather specific and dissociable performance deficits. Signals along the superior path appear to be specialized for action or spatial orientation; signals along the inferior path appear to be specialized for object recognition (Milner and Goodale, 2006; Ungerleider and Mishkin, 1982). (*Brain image courtesy of Dr. Ugur Ture.*) (B) Signals between visual field maps are carried along pathways whose axons terminate in distinct patterns. These termination patterns can be classified into ascending, descending and lateral connectivity and establish a hierarchical representation (Felleman and Essen, 1991; Van Essen and Maunsell, 1983). The hierarchy between a subset of the maps is shown here. (This figure based upon (Barone et al., 2000, Fig. 11)).

Figure 9. Visual field map clusters. A schematic diagram of the organization of eccentricity representations in visual cortex is shown at the top. The image shows the visual field map grouped into clusters, as they appear on flattened cortex. The concentric colored circles designate the eccentricity representations of maps within a cluster. Each cluster contains several visual field maps that can be delineated based on the angle maps. Eccentricity measurements spanning 0-11° are shown on a flattened section of cortex (bottom). Dotted lines overlaid on the flattened data illustrate the clusters. Color legend (bottom right) shows the

eccentricity that most effectively drives each cortical location. The bottom image is cropped to show only the data within defined visual field maps. VO: ventral-occipital, LO: lateral-occipital.

Figure 10. Computational models to estimate the neural responses driving the BOLD signal. Recent modeling efforts have focused on creating a neural model (top box) that predicts the BOLD response to any stimulus (Dumoulin and Wandell, in press). The neural model combines a model of certain neural properties along with a model of nuisance factors, such as the hemodynamic response, eye movements, and so forth. The prediction is compared with the BOLD data at each location in cortex. The neuronal model parameters are adjusted to minimize the difference between the prediction and the data. As the solution converges, the neural model parameters are output for analysis.

References

Albright, T. D., Desimone, R., and Gross, C. G. (1984). Columnar organization of directionally selective cells in visual area MT of the macaque. J Neurophysiol *51*, 16-31.

Allman, J. M., and Kaas, J. H. (1971). A representation of the visual field in the caudal third of the middle temporal gyrus of the owl monkey. Brain Research *31*, 85-105.

Amunts, K., Malikovic, A., Mohlberg, H., Schormann, T., and Zilles, K. (2000). Brodmann's areas 17 and 18 brought into stereotaxic space-where and how variable? Neuroimage *11*, 66-84.

Baizer, J. S., Ungerleider, L. G., and Desimone, R. (1991). Organization of visual inputs to the inferior temporal and posterior parietal cortex in macaques. J Neurosci *11*, 168-190.

Barbas, H., and Rempel-Clower, N. (1997). Cortical structure predicts the pattern of corticocortical connections. Cereb Cortex *7*, 635-646.

Barnes, G. R., Hess, R. F., Dumoulin, S. O., Achtman, R. L., and Pike, G. B. (2001). The cortical deficit in humans with strabismic amblyopia. J Physiol *533*, 281-297.

Barone, P., Batardiere, A., Knoblauch, K., and Kennedy, H. (2000). Laminar distribution of neurons in extrastriate areas projecting to visual areas V1 and V4 correlates with the hierarchical rank and indicates the operation of a distance rule. J Neurosci *20*, 3263-3281.

Baseler, H. A., Brewer, A. A., Sharpe, L. T., Morland, A. B., Jagle, H., and Wandell, B. A. (2002). Reorganization of human cortical maps caused by inherited photoreceptor abnormalities. Nat Neurosci *5*, 364-370.

Baseler, H. A., Morland, A. B., and Wandell, B. A. (1999). Topographic organization of human visual areas in the absence of input from primary cortex. J Neurosci *19*, 2619-2627.

Beauchamp, M. S., Yasar, N. E., Kishan, N., and Ro, T. (2007). Human MST but not MT responds to tactile stimulation. J Neurosci *27*, 8261-8267.

Blinkov, S., and Glezer, I. (1968). The human brain in figures and tables, Plenum).

Bourne, J. A., and Rosa, M. G. (2003). Neurofilament protein expression in the geniculostriate pathway of a New World monkey (Callithrix jacchus). Exp Brain Res *150*, 19-24.

Braitenberg, V., and Schüz, A. (1998). Cortex: Statistics and Geometry of Neuronal Connectivity, 2nd edn).

Brewer, A. A., Liu, J., Wade, A. R., and Wandell, B. A. (2005). Visual field maps and stimulus selectivity in human ventral occipital cortex. Nat Neurosci *8*, 1102-1109.

Brewer, A. A., Press, W. A., Logothetis, N. K., and Wandell, B. A. (2002). Visual areas in macaque cortex measured using functional magnetic resonance imaging. J Neurosci *22*, 10416-10426.

Brindley, G. S., and Lewin, W. S. (1968). The sensations produced by electrical stimulation of the visual

cortex. J Physio *196*, 479-493.
Buracas, G. T., and Boynton, G. M. (2002). Efficient design of event-related fMRI experiments using M-sequences. Neuroimage *16*, 801-813.
Burkhalter, A., Felleman, D. J., Newsome, W. T., and Essen, D. C. V. (1986). Anatomical and physiological asymmetries related to visual areas {V3} and {VP} in macaque extrastriate cortex. Vision Research *26*, 63-80.
Collins, D. L., Neelin, P., Peters, T. M., and Evans, A. C. (1994). Automatic 3D intersubject registration of MR volumetric data in standardized Talairach space. J Comput Assist Tomogr *18*, 192-205.
d'Avossa, G., Tosetti, M., Crespi, S., Biagi, L., Burr, D. C., and Morrone, M. C. (2007). Spatiotopic selectivity of BOLD responses to visual motion in human area MT. Nat Neurosci *10*, 249-255.
Daniel, P. M., and Whitteridge, D. (1961). The representation of the visual field on the cerebral cortex in monkeys. J Physiol, Lond *159*, 203-221.
DeSouza, J. F., Dukelow, S. P., and Vilis, T. (2002). Eye position signals modulate early dorsal and ventral visual areas. Cereb Cortex *12*, 991-997.
DeYoe, E. A., Carman, G. J., Bandettini, P., Glickman, S., Wieser, J., Cox, R., Miller, D., and Neitz, J. (1996). Mapping striate and extrastriate visual areas in human cerebral cortex. Proc Natl Acad Sci (USA) *93*, 2382-2386.
Di Russo, F., Martinez, A., Sereno, M. I., Pitzalis, S., and Hillyard, S. A. (2002). Cortical sources of the early components of the visual evoked potential. Hum Brain Mapp *15*, 95-111.
Dougherty, R. F., Ben-Shachar, M., Bammer, R., Brewer, A. A., and Wandell, B. A. (2005). Functional organization of human occipital-callosal fiber tracts. Proc Natl Acad Sci U S A *102*, 7350-7355.
Dougherty, R. F., Koch, V. M., Brewer, A. A., Fischer, B., Modersitzki, J., and Wandell, B. A. (2003). Visual field representations and locations of visual areas V1/2/3 in human visual cortex. J Vis *3*, 586-598.
Dukelow, S. P., DeSouza, J. F., Culham, J. C., van den Berg, A. V., Menon, R. S., and Vilis, T. (2001). Distinguishing subregions of the human MT+ complex using visual fields and pursuit eye movements. J Neurophysiol *86*, 1991-2000.
Dumoulin, S. O., Bittar, R. G., Kabani, N. J., Baker, C. L., Jr., Le Goualher, G., Bruce Pike, G., and Evans, A. C. (2000). A new anatomical landmark for reliable identification of human area V5/MT: a quantitative analysis of sulcal patterning. Cereb Cortex *10*, 454-463.
Dumoulin, S. O., Hoge, R. D., Baker, C. L., Jr., Hess, R. F., Achtman, R. L., and Evans, A. C. (2003). Automatic volumetric segmentation of human visual retinotopic cortex. Neuroimage *18*, 576-587.
Dumoulin, S. O., and Wandell, B. A. (in press). Population receptive field estimates in human visual cortex. Neuroimage.
Ejima, Y., Takahashi, S., Yamamoto, H., Fukunaga, M., Tanaka, C., Ebisu, T., and Umeda, M. (2003). Interindividual and interspecies variations of the extrastriate visual cortex. Neuroreport *14*, 1579-1583.
Engel, S. A., Glover, G. H., and Wandell, B. A. (1997). Retinotopic organization in human visual cortex and the spatial precision of functional MRI. Cereb Cortex *7*, 181-192.
Engel, S. A., Rumelhart, D. E., Wandell, B. A., Lee, A. T., Glover, G. H., Chichilnisky, E. J., and Shadlen, M. N. (1994). fMRI of human visual cortex [letter] [published erratum appears in Nature 1994 Jul 14;370(6485):106]. Nature *369*, 525.
Essen, D. C. V., Newsome, W. T., and Maunsell, J. H. R. (1984). The visual field representation in striate cortex of the Macaque monkey: Asymmetries, anisotropies and individual variability. Vision Res *24*, 429-448.
Felleman, D. J., and Essen, D. C. V. (1991). Distributed hierarchical processing in the primate cerebral cortex. Cerebral Cortex *1*, 1-47.
Fischl, B., and Dale, A. M. (2000). Measuring the thickness of the human cerebral cortex from magnetic resonance images. Proc Natl Acad Sci U S A *97*, 11050-11055.
Fishman, R. S. (1997). Gordon Holmes, the cortical retina, and the wounds of war. The seventh Charles B. Snyder Lecture. Doc Ophthalmol *93*, 9-28.
Fize, D., Vanduffel, W., Nelissen, K., Denys, K., Chef d'Hotel, C., Faugeras, O., and Orban, G. A. (2003). The retinotopic organization of primate dorsal V4 and surrounding areas: A functional magnetic resonance

imaging study in awake monkeys. J Neurosci *23*, 7395-7406.
Fox, P. T., Miezin, F. M., Allman, J. M., Van Essen, D. C., and Raichle, M. E. (1987). Retinotopic organization of human visual cortex mapped with positron- emission tomography. J Neurosci *7*, 913-922.
Friston, K. J., Rotshtein, P., Geng, J. J., Sterzer, P., and Henson, R. N. (2006). A critique of functional localisers. Neuroimage *30*, 1077-1087.
Galletti, C., Fattori, P., Battaglini, P. P., Shipp, S., and Zeki, S. (1996). Functional demarcation of a border between areas V6 and V6A in the superior parietal gyrus of the macaque monkey. Eur J Neurosci *8*, 30-52.
Galletti, C., Fattori, P., Gamberini, M., and Kutz, D. F. (1999). The cortical visual area V6: brain location and visual topography. Eur J Neurosci *11*, 3922-3936.
Gardner, J. L., Sun, P., Waggoner, R. A., Ueno, K., Tanaka, K., and Cheng, K. (2005). Contrast adaptation and representation in human early visual cortex. Neuron *47*, 607-620.
Goodale, M. A., and Milner, A. D. (1992). Separate visual pathways for perception and action. Trends Neurosci *15*, 20-25.
Goossens, J., Dukelow, S. P., Menon, R. S., Vilis, T., and van den Berg, A. V. (2006). Representation of head-centric flow in the human motion complex. J Neurosci *26*, 5616-5627.
Grill-Spector, K., and Malach, R. (2004). The human visual cortex. Annu Rev Neurosci *27*, 649-677.
Grinvald, A. (1985). Real-time optical mapping of neuronal activity: From single growth cones to the intact mammalian brain. Ann Rev Neurosci *8*, 263-305.
Hadjikhani, N., Liu, A. K., Dale, A. M., Cavanagh, P., and Tootell, R. B. H. (1998). Retinotopy and color sensitivity in human visual cortical area V8. Nature Neuroscience *1*, 235 - 241.
Hagler, D. J., Jr., Riecke, L., and Sereno, M. I. (2007). Parietal and superior frontal visuospatial maps activated by pointing and saccades. Neuroimage *35*, 1562-1577.
Hagler, D. J., Jr., and Sereno, M. I. (2006). Spatial maps in frontal and prefrontal cortex. Neuroimage *29*, 567-577.
Hansen, K. A., David, S. V., and Gallant, J. L. (2004). Parametric reverse correlation reveals spatial linearity of retinotopic human V1 BOLD response. Neuroimage *23*, 233-241.
Hasson, U., Harel, M., Levy, I., and Malach, R. (2003). Large-scale mirror-symmetry organization of human occipito-temporal object areas. Neuron *37*, 1027-1041.
Hasson, U., Levy, I., Behrmann, M., Hendler, T., and Malach, R. (2002). Eccentricity bias as an organizing principle for human high-order object areas. Neuron *34*, 479-490.
Helmholtz, H. (1896). Physiological Optics.
Holmes, G. (1918). Distrubances of vision by cerebral lesions. Bre J Opthal *2*, 353-384.
Horton, J. C., and Hoyt, W. F. (1991). Quadrantic visual field defects: a hallmark of lesions in extrastriate (V2/V3) cortex. Brain *114*, 1703-1718.
Hubel, D. H., and Wiesel, T. N. (1965). Receptive Fields and Functional Architecture in Two Nonstriate Visual Areas (18 and 19) of the Cat. J Neurophysiol *28*, 229-289.
Huk, A. C., Dougherty, R. F., and Heeger, D. J. (2002). Retinotopy and functional subdivision of human areas MT and MST. J Neurosci *22*, 7195-7205.
Iaria, G., and Petrides, M. (2007). Occipital sulci of the human brain: variability and probability maps. J Comp Neurol *501*, 243-259.
Inouye, T. (1909). Die Sehstroungen bei Schussverietzungen der kortikalen Sehsphare (Leipzig, Germany, W. Engelmann).
Jack, A. I., Patel, G. H., Astafiev, S. V., Snyder, A. Z., Akbudak, E., Shulman, G. L., and Corbetta, M. (2007). Changing human visual field organization from early visual to extra-occipital cortex. PLoS ONE *2*, e452.
Kanwisher, N., McDermott, J., and Chun, M. M. (1997). The fusiform face area: a module in human extrastriate cortex specialized for face perception. J Neurosci *17*, 4302-4311.
Kastner, S., DeSimone, K., Konen, C. S., Szczepanski, S. M., Weiner, K. S., and Schneider, K. A. (2007). Topographic maps in human frontal cortex revealed in memory-guided saccade and spatial working-memory tasks. J Neurophysiol *97*, 3494-3507.
Larsson, J., and Heeger, D. J. (2006). Two retinotopic visual areas in human lateral occipital cortex. J

Neurosci *26*, 13128-13142.
Larsson, J., Landy, M. S., and Heeger, D. J. (2006). Orientation-selective adaptation to first- and second-order patterns in human visual cortex. J Neurophysiol *95*, 862-881.
Levy, I., Hasson, U., Avidan, G., Hendler, T., and Malach, R. (2001). Center-periphery organization of human object areas. Nat Neurosci *4*, 533-539.
Li, X., Dumoulin, S. O., Mansouri, B., and Hess, R. F. (2007). The fidelity of the cortical retinotopic map in human amblyopia. Eur J Neurosci *25*, 1265-1277.
Logothetis, N. K. (2002). The neural basis of the BOLD fMRI signal. Philosophical Transactions of the Royal Society Series B (London) *357*, 1003-1037.
Lyon, D. C., and Kaas, J. H. (2002). Evidence for a modified V3 with dorsal and ventral halves in macaque monkeys. Neuron *33*, 453-461.
Malach, R., Reppas, J. B., Benson, R. R., Kwong, K. K., Jiang, H., Kennedy, W. A., Ledden, P. J., Brady, T. J., Rosen, B. R., and Tootell, R. B. (1995). Object-related activity revealed by functional magnetic resonance imaging in human occipital cortex. Proc Natl Acad Sci U S A *92*, 8135-8139.
McKeefry, D. J., and Zeki, S. (1997). The position and topography of the human colour centre as revealed by functional magnetic resonance imaging. Brain *120*, 2229-2242.
McKyton, A., and Zohary, E. (2007). Beyond retinotopic mapping: the spatial representation of objects in the human lateral occipital complex. Cereb Cortex *17*, 1164-1172.
Merabet, L. B., Swisher, J. D., McMains, S. A., Halko, M. A., Amedi, A., Pascual-Leone, A., and Somers, D. C. (2007). Combined activation and deactivation of visual cortex during tactile sensory processing. J Neurophysiol *97*, 1633-1641.
Milner, A. D., and Goodale, M. A. (2006). The Visual Brain in Action, 2nd edn, Oxford University Press).
Montaser-Kouhsari, L., Landy, M. S., Heeger, D. J., and Larsson, J. (2007). Orientation-selective adaptation to illusory contours in human visual cortex. J Neurosci *27*, 2186-2195.
Morland, A. B., Baseler, H. A., Hoffmann, M. B., Sharpe, L. T., and Wandell, B. A. (2001). Abnormal retinotopic representations in human visual cortex revealed by fMRI. Acta Psychol (Amst) *107*, 229-247.
Newton, I. (1704). Opticks: A Treatise of the Reflections Refractions, Inflections and Colours of Light, 4th edn (London, Printed for William Innys at the West End of St. Paul's).
Ogawa, S., and Lee, T. M. (1990). Magnetic resonance imaging of blood vessels at high fields: in vivo and in vitro measurements and image simulation. Magn Reson Med *16*, 9-18.
Ogawa, S., Lee, T. M., Nayak, A. S., and Glynn, P. (1990). Oxygenation-sensitive contrast in magnetic resonance image of rodent brain at high magnetic fields. Magn Reson Med *14*, 68-78.
Ogawa, S., Tank, D., Menon, R., Ellermann, J., Kim, S., Merkle, H., and Ugurbil, K. (1992). Intrinsic signal changes accompanying sensory stimulation: Functional brain mapping with magnetic resonance imaging. Proc Nat Acad Sci *89*, 591-5955.
Pandya, D. N., Seltzer, B., and Barbas, H. (1988). Input-Output organization of the primate cerebral cortex. In Comparative Primate Biology, H. D. Staklis, and J. Erwin, eds. (New York, Alan R. Liss), pp. 39-80.
Pitzalis, S., Galletti, C., Huang, R. S., Patria, F., Committeri, G., Galati, G., Fattori, P., and Sereno, M. I. (2006). Wide-field retinotopy defines human cortical visual area v6. J Neurosci *26*, 7962-7973.
Press, W. A., Brewer, A. A., Dougherty, R. F., Wade, A. R., and Wandell, B. A. (2001). Visual areas and spatial summation in human visual cortex. Vision Research *41*, 1321-1332.
Rademacher, J., Caviness, V. S., Jr., Steinmetz, H., and Galaburda, A. M. (1993). Topographical variation of the human primary cortices: implications for neuroimaging, brain mapping, and neurobiology. Cereb Cortex *3*, 313-329.
Rosa, M. G., and Tweedale, R. (2005). Brain maps, great and small: lessons from comparative studies of primate visual cortical organization. Philos Trans R Soc Lond B Biol Sci *360*, 665-691.
Salzman, C. D., Britten, K. H., and Newsome, W. T. (1990). Cortical microstimulation influences perceptual judgements of motion direction. Nature *346*, 174-177.
Salzman, C. D., Murasugi, C. M., Britten, K. H., and Newsome, W. T. (1992). Microstimulation in Visual Area MT: Effects on Direction Discrimination Performance. Paper presented at: J. Neuroscience.
Saxe, R., Brett, M., and Kanwisher, N. (2006). Divide and conquer: a defense of functional localizers.

Neuroimage *30*, 1088-1096; discussion 1097-1089.
Schluppeck, D., Glimcher, P., and Heeger, D. J. (2005). Topographic organization for delayed saccades in human posterior parietal cortex. J Neurophysiol *94*, 1372-1384.
Schneider, G. E. (1969). Two visual systems. Science *163*, 895-902.
Schneider, W., Noll, D. C., and Cohen, J. D. (1993). Functional topographic mapping of the cortical ribbon in human vision with conventional MRI scanners. Nature *365*, 150-153.
Schwartz, E. L. (1977). Spatial mapping in the primate sensory projection: analytic structure and relevance to perception. Biol Cybern *25*, 181-194.
Sereno, M. I., Dale, A. M., Reppas, J. B., Kwong, K. K., Belliveau, J. W., Brady, T. J., Rosen, B. R., and Tootell, R. B. (1995). Borders of multiple human visual areas in humans revealed by functional mri. Science *268*, 889-893.
Sereno, M. I., Pitzalis, S., and Martinez, A. (2001). Mapping of contralateral space in retinotopic coordinates by a parietal cortical area in humans. Science *294*, 1350-1354.
Shepard, R. N. (1981). Psychophysical complementarity. In Perceptual Organization, M. K. a. J. Pomerantz, ed. (N.J.), pp. 279-341.
Shepard, R. N. (2001). Perceptual-cognitive universals as reflections of the world. Behav Brain Sci *24*, 581-601; discussion 652-571.
Sherman, S. M., and Guillery, R. W. (2001). Exploring the Thalamus, Academic Press).
Shipp, S., Watson, J. D., Frackowiak, R. S., and Zeki, S. (1995). Retinotopic maps in human prestriate visual cortex: the demarcation of areas V2 and V3. Neuroimage *2*, 125-132.
Silver, M. A., Ress, D., and Heeger, D. J. (2005). Topographic maps of visual spatial attention in human parietal cortex. J Neurophysiol *94*, 1358-1371.
Sincich, L. C., Park, K. F., Wohlgemuth, M. J., and Horton, J. C. (2004). Bypassing V1: a direct geniculate input to area MT. Nat Neurosci *7*, 1123-1128.
Smith, A. T., Greenlee, M. W., Singh, K. D., Kraemer, F. M., and Hennig, J. (1998). The processing of first- and second-order motion in human visual cortex assessed by functional magnetic resonance imaging (fMRI). J Neurosci *18*, 3816-3830.
Smith, A. T., Singh, K. D., Williams, A. L., and Greenlee, M. W. (2001). Estimating receptive field size from fMRI data in human striate and extrastriate visual cortex. Cereb Cortex *11*, 1182-1190.
Smith, A. T., Wall, M. B., Williams, A. L., and Singh, K. D. (2006). Sensitivity to optic flow in human cortical areas MT and MST. Eur J Neurosci *23*, 561-569.
Stenbacka, L., and Vanni, S. (2007). fMRI of peripheral visual field representation. Clin Neurophysiol *118*, 1303-1314.
Stensaas, S. S., Eddington, D. K., and Dobelle, W. H. (1974). The topography and variability of the primary visual cortex in man. J Neurosurg *40*, 747-755.
Sutter, E. E., and Tran, D. (1992). The field topography of ERG components in man--I. The photopic luminance response. Vision Res *32*, 433-446.
Swisher, J. D., Halko, M. A., Merabet, L. B., McMains, S. A., and Somers, D. C. (2007). Visual topography of human intraparietal sulcus. J Neurosci *27*, 5326-5337.
Talairach, J., and Tournoux, P. (1988). Col-Planar Stereotax Atlast of the Human Brain (New York, Thieme Medical Publishers).
Talbot, S., and Marshall, W. (1941). Physiological studies on neural mechanisms of visual localization and discrimination. Am J Ophthalmol *24*, 1255-1263.
Talbot, S. A. (1940). Arrangement of visual field on cat's cortex. Am J Physiol *129*, 477-478.
Talbot, S. A. (1942). A lateral localization in the cat's visual cortex. Fed Proc *1*, 84.
Teuber, H. L., Battersby, W. S., and Bender, M. B. (1960). Visual Field Defects After Penetrating Missile Wounds of the Brain (Cambridge, Mass.).
Thirion, B., Duchesnay, E., Hubbard, E., Dubois, J., Poline, J. B., Lebihan, D., and Dehaene, S. (2006). Inverse retinotopy: inferring the visual content of images from brain activation patterns. Neuroimage *33*, 1104-1116.
Thompson, J. M., Woolsey, C. N., and Talbot, S. A. (1950). Visual areas I and II of cerebral cortex of rabbit.

J Neurophysio *12*, 277·288.
Thompson, P. M., Schwartz, C., Lin, R. T., Khan, A. A., and Toga, A. W. (1996). Three-dimensional statistical analysis of sulcal variability in the human brain. J Neurosci *16*, 4261-4274.
Tootell, R. B., and Hadjikhani, N. (2001). Where is 'dorsal V4' in human visual cortex? Retinotopic, topographic and functional evidence. Cereb Cortex *11*, 298-311.
Tootell, R. B., Hadjikhani, N., Hall, E. K., Marrett, S., Vanduffel, W., Vaughan, J. T., and Dale, A. M. (1998). The retinotopy of visual spatial attention. Neuron *21*, 1409-1422.
Tootell, R. B., Mendola, J. D., Hadjikhani, N. K., Ledden, P. J., Liu, A. K., Reppas, J. B., Sereno, M. I., and Dale, A. M. (1997). Functional analysis of V3A and related areas in human visual cortex, Vol 17).
Tootell, R. B., Reppas, J. B., Kwong, K. K., Malach, R., Born, R. T., Brady, T. J., Rosen, B. R., and Belliveau, J. W. (1995). Functional analysis of human MT and related visual cortical areas using magnetic resonance imaging. J Neurosci *15*, 3215-3230.
Trevarthen, C. B. (1968). Two mechanisms of vision in primates. Psychol Forsch *31*, 299-348.
Tusa, R. J., Palmer, L. A., and Rosenquist, A. C. (1978). The retinotopic organization of area 17 (striate cortex) in the cat. J Comp Neurol *177*, 213-235.
Ungerleider, L. G., and Mishkin, M. (1982). Two Cortical Visual Systems. In The Analysis of Visual Behavior, D. J. I. a. R. J. W. M. a. M. S. Goodale, ed. (Cambridge), pp. 549-586.
Van Essen, D. C. (2002). Surface-based atlases of cerebellar cortex in the human, macaque, and mouse. Ann N Y Acad Sci *978*, 468-479.
Van Essen, D. C. (2003). Organization of Visual Areas in Macaque and Human Cerebral Cortex. In The Visual Neurosciences, L. M. Chalupa, and J. S. Werner, eds. (Boston, Bradford Books).
Van Essen, D. C. (2005). A Population-Average, Landmark- and Surface-based (PALS) atlas of human cerebral cortex. Neuroimage *28*, 635-662.
Van Essen, D. C. (in press). Evolution of Nervous Systems. Neuroimage.
Van Essen, D. C., and Maunsell, J. H. (1983). Hierarchical organization and functional streams in the visual cortex. Trends in Neuroscience, 370-375.
Vanni, S., Henriksson, L., and James, A. C. (2005). Multifocal fMRI mapping of visual cortical areas. Neuroimage *27*, 95-105.
Victor, J. D., Apkarian, P., Hirsch, J., Conte, M. M., Packard, M., Relkin, N. R., Kim, K. H., and Shapley, R. M. (2000). Visual function and brain organization in non-decussating retinal-fugal fibre syndrome. Cereb Cortex *10*, 2-22.
Wade, A. R., Brewer, A. A., Rieger, J. W., and Wandell, B. A. (2002). Functional measurements of human ventral occipital cortex: retinotopy and colour. Philos Trans R Soc Lond B Biol Sci *357*, 963-973.
Wandell, B. A. (1995). Foundations of Vision (Sunderland, MA, Sinauer Press).
Wandell, B. A., Brewer, A. A., and Dougherty, R. F. (2005). Visual field map clusters in human cortex. Philos Trans R Soc Lond B Biol Sci *360*, 693-707.
Wandell, B. A., Dumoulin, S. O., and Brewer, A. A. (2006). Computational neuroimaging: Color signals in the visual pathways. Neuro-opthalmol Jpn *23* 324-343.
Wandell, B. A., Dumoulin, S. O., and Brewer, A. A. (in press). Visual areas in humans. In The New Encyclopedia of Neuroscience, L. S. e. al., ed. (Oxford, England, Elsevier).
Warnking, J., Dojat, M., Guerin-Dugue, A., Delon-Martin, C., Olympieff, S., Richard, N., Chehikian, A., and Segebarth, C. (2002). fMRI retinotopic mapping--step by step. Neuroimage *17*, 1665-1683.
Watson, J. D., Myers, R., Frackowiak, R. S., Hajnal, J. V., Woods, R. P., Mazziotta, J. C., Shipp, S., and Zeki, S. (1993). Area V5 of the human brain: evidence from a combined study using positron emission tomography and magnetic resonance imaging. Cereb Cortex *3*, 79-94.
Yoshor, D., Bosking, W. H., Ghose, G. M., and Maunsell, J. H. (2007). Receptive fields in human visual cortex mapped with surface electrodes. Cereb Cortex *17*, 2293-2302.
Young, M. P. (1992). Objective analysis of the topological organization of the primate cortical visual system. Nature *358*, 152-155.
Zeki, S. (1980). The response properties of cells in the middle temporal area (area MT) of owl monkey visual cortex. Proc R Soc Lond B Biol Sci *207*, 239-248.

Zeki, S. (1990). Parallelism and Functional Specialization in Human Visual Cortex. Cold Spring Harbor Symposia on Quantitative Biology *55*, 651-661.
Zeki, S. (1993). A Vision of the Brain (London, Blackwell Scientific Publications).
Zeki, S. (2003). Improbable areas in the visual brain. Trends Neurosci *26*, 23-26.
Zeki, S., McKeefry, D. J., Bartels, A., and Frackowiak, R. S. (1998). Has a new color area been discovered? Nat Neurosci *1*, 335-336.
Zeki, S., Watson, J. D., Lueck, C. J., Friston, K. J., Kennard, C., and Frackowiak, R. S. (1991). A direct demonstration of functional specialization in human visual cortex. J Neurosci *11*, 641-649.

A

B

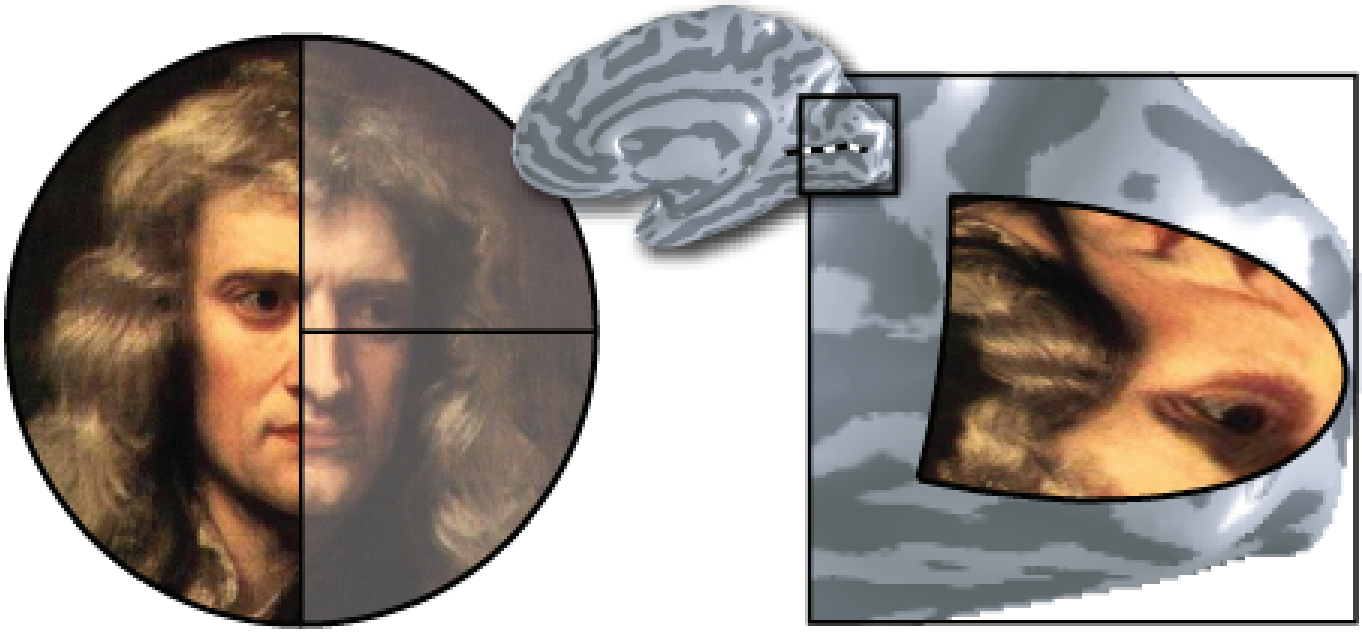

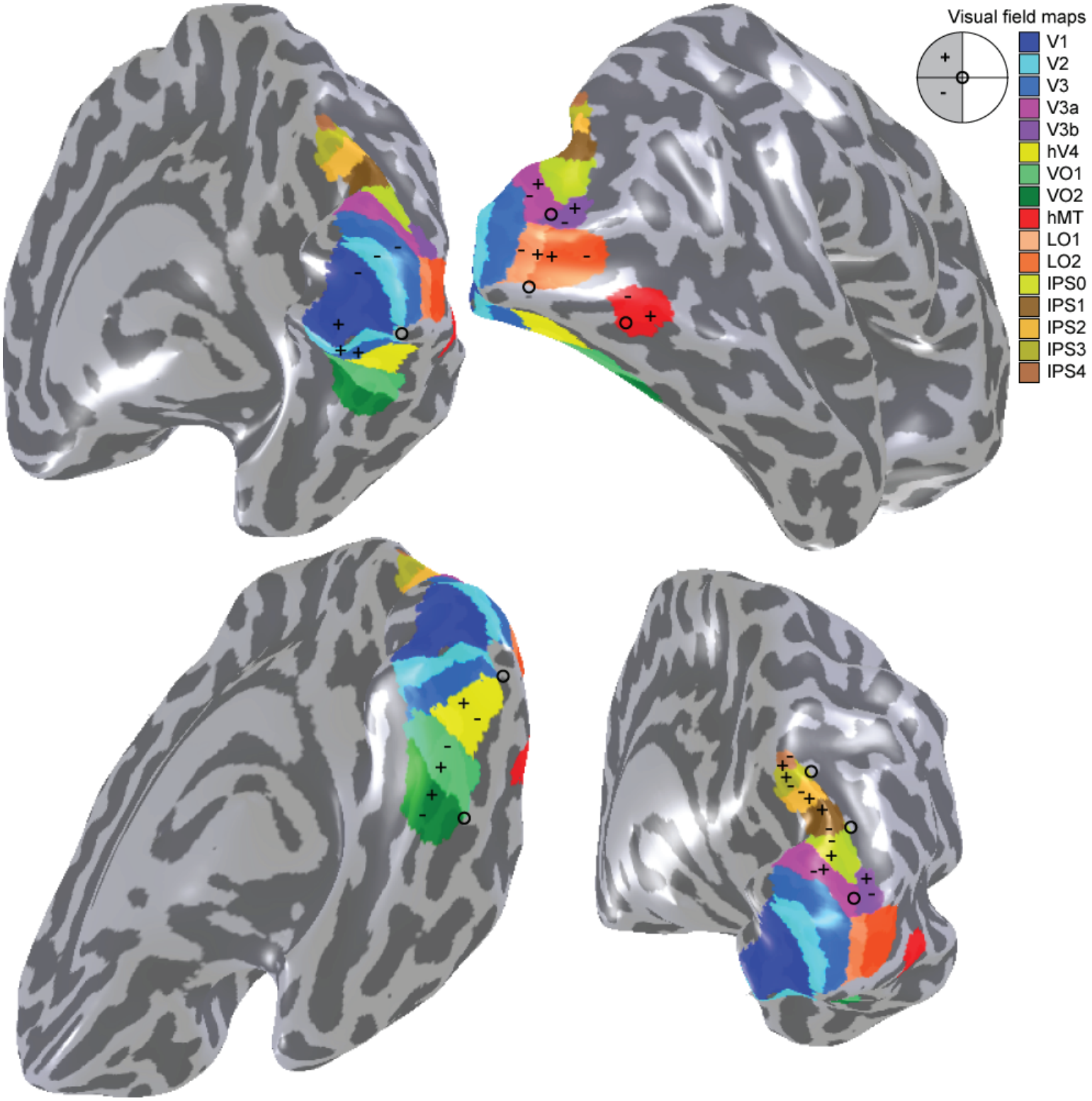
Visual field maps
V1
V2
V3
V3a
V3b
hV4
VO1
VO2
hMT
LO1
LO2
IPS0
IPS1
IPS2
IPS3
IPS4

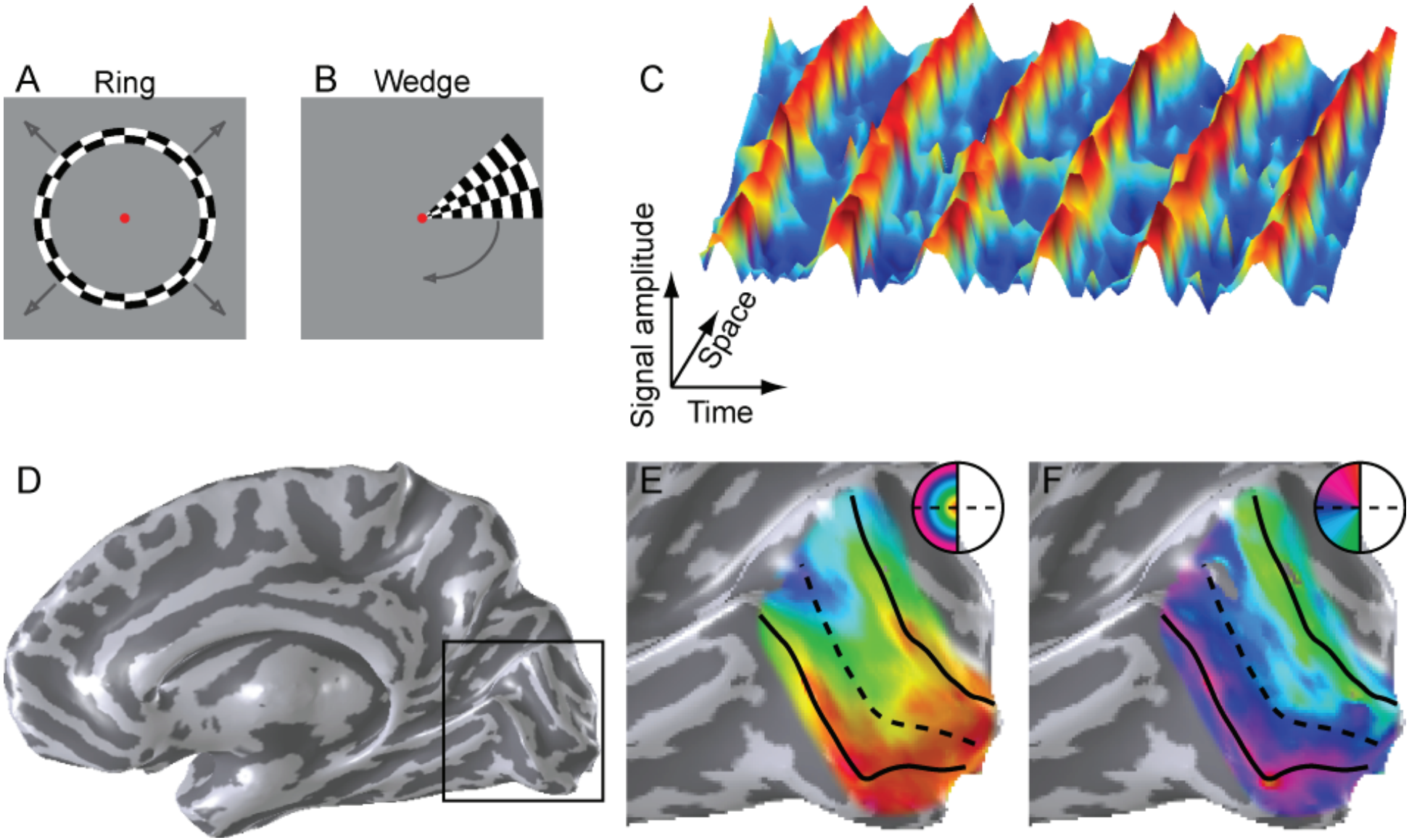
A
Ring
B
Wedge
C
Signal amplitude
Space
Time
D
E
F

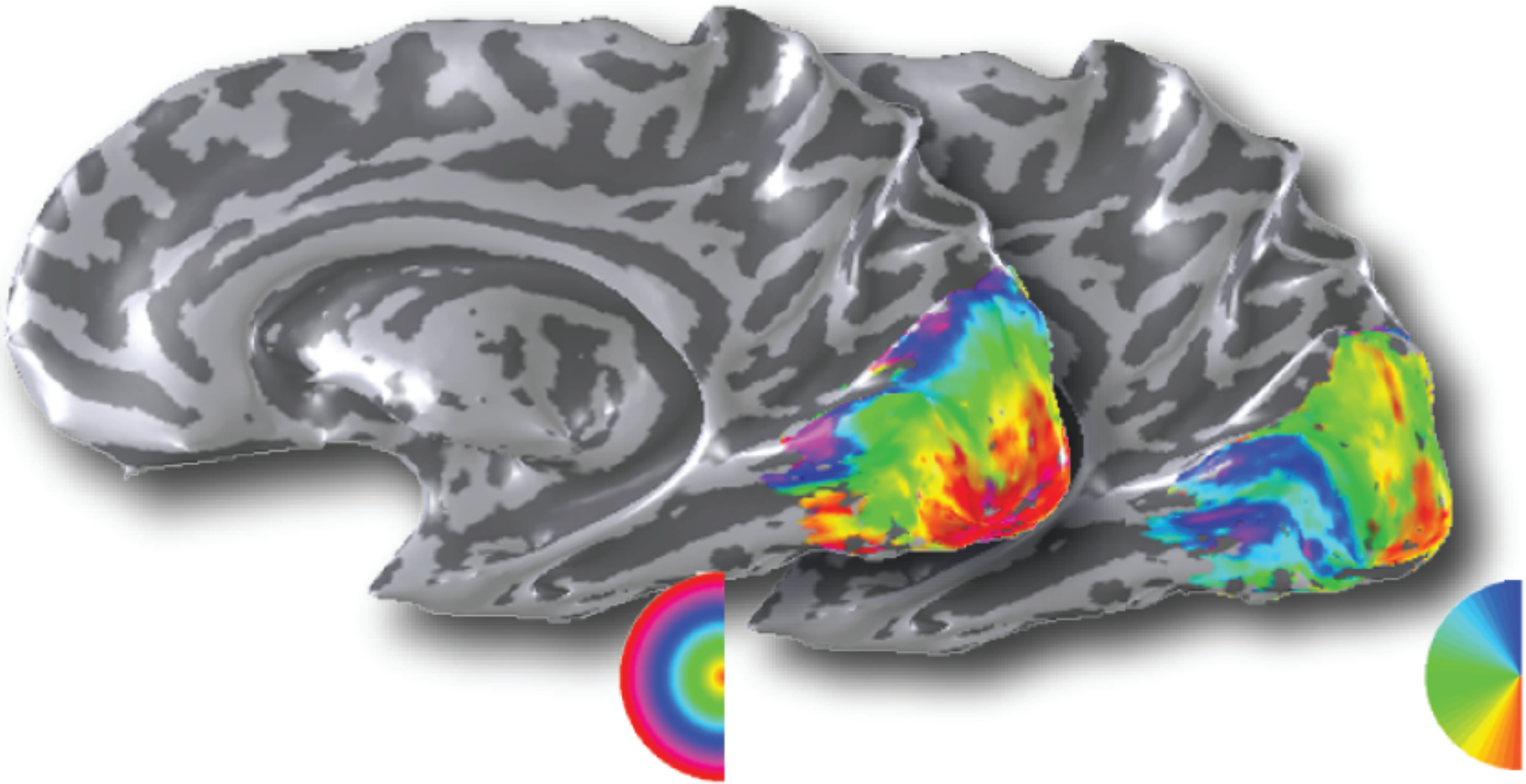
20 deg

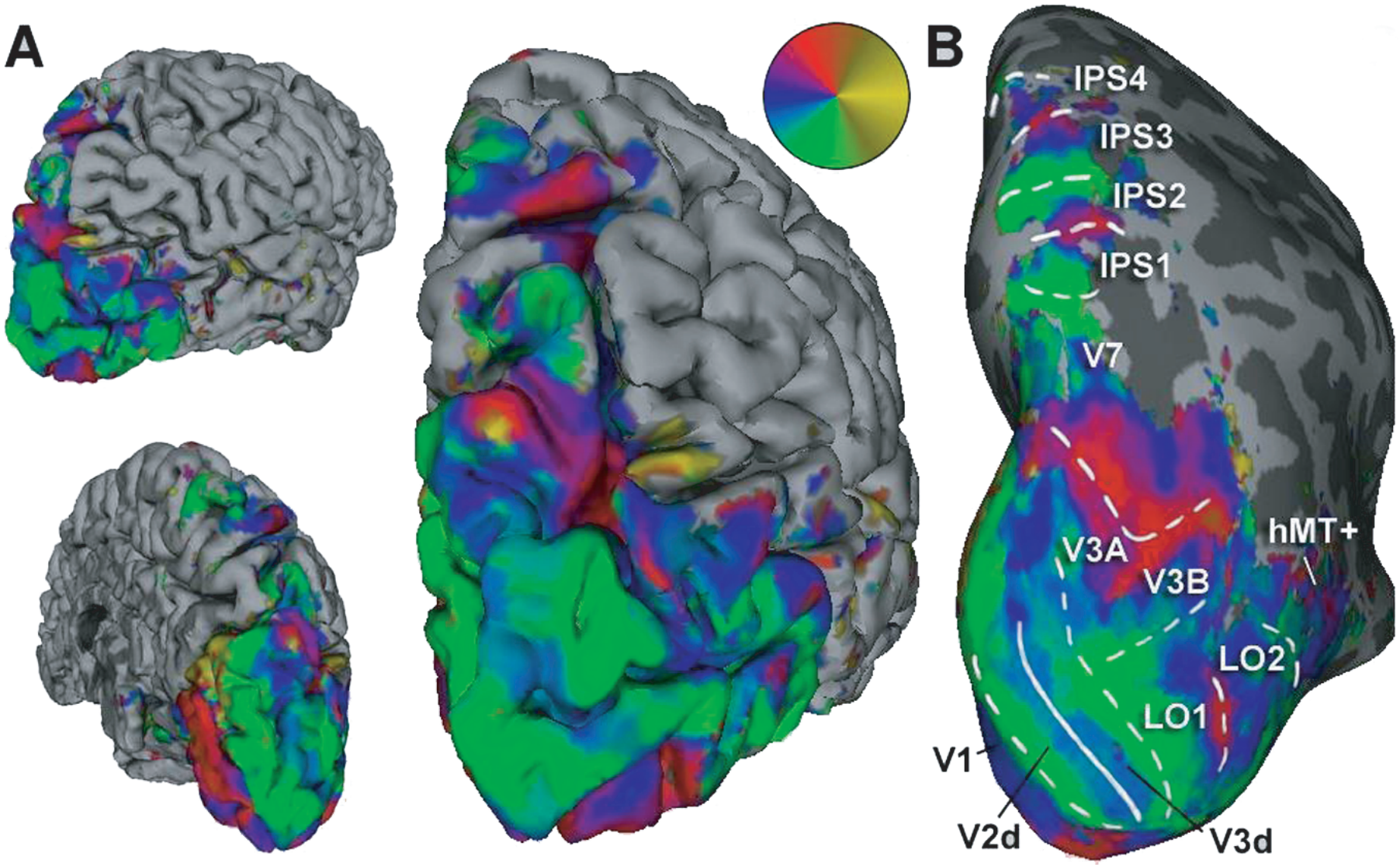
A
B
IPS4
IPS3
IPS2
IPS1
V7
V3A
V3B
hMT+
LO2
LO1
V1
V2d
V3d

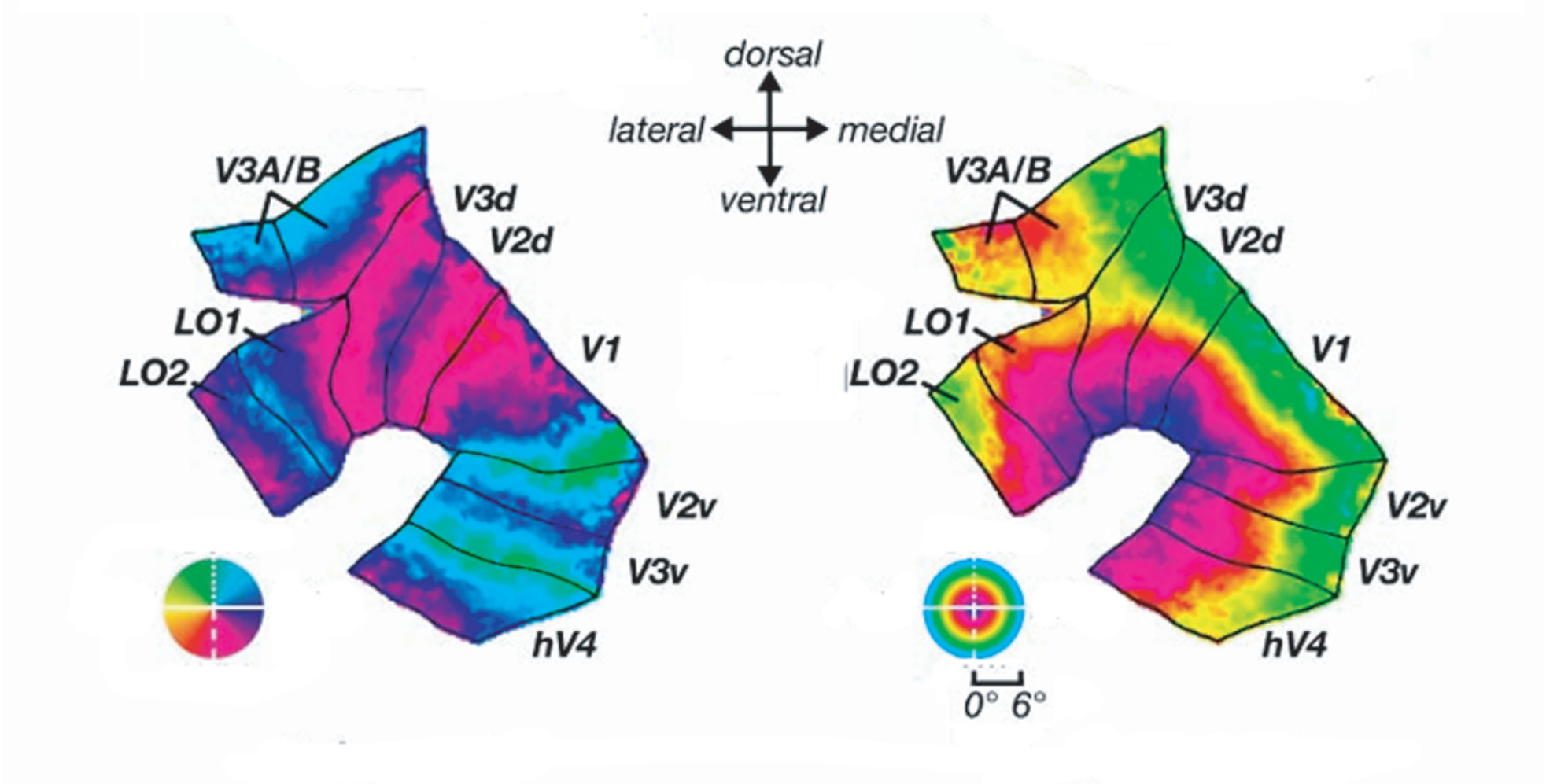
dorsal
lateral
medial
ventral
V3A/B
V3d
V2d
LO1
LO2
V1
V2v
V3v
hV4
V3A/B
V3d
V2d
LO1
LO2
V1
V2v
V3v
hV4
0° 6°

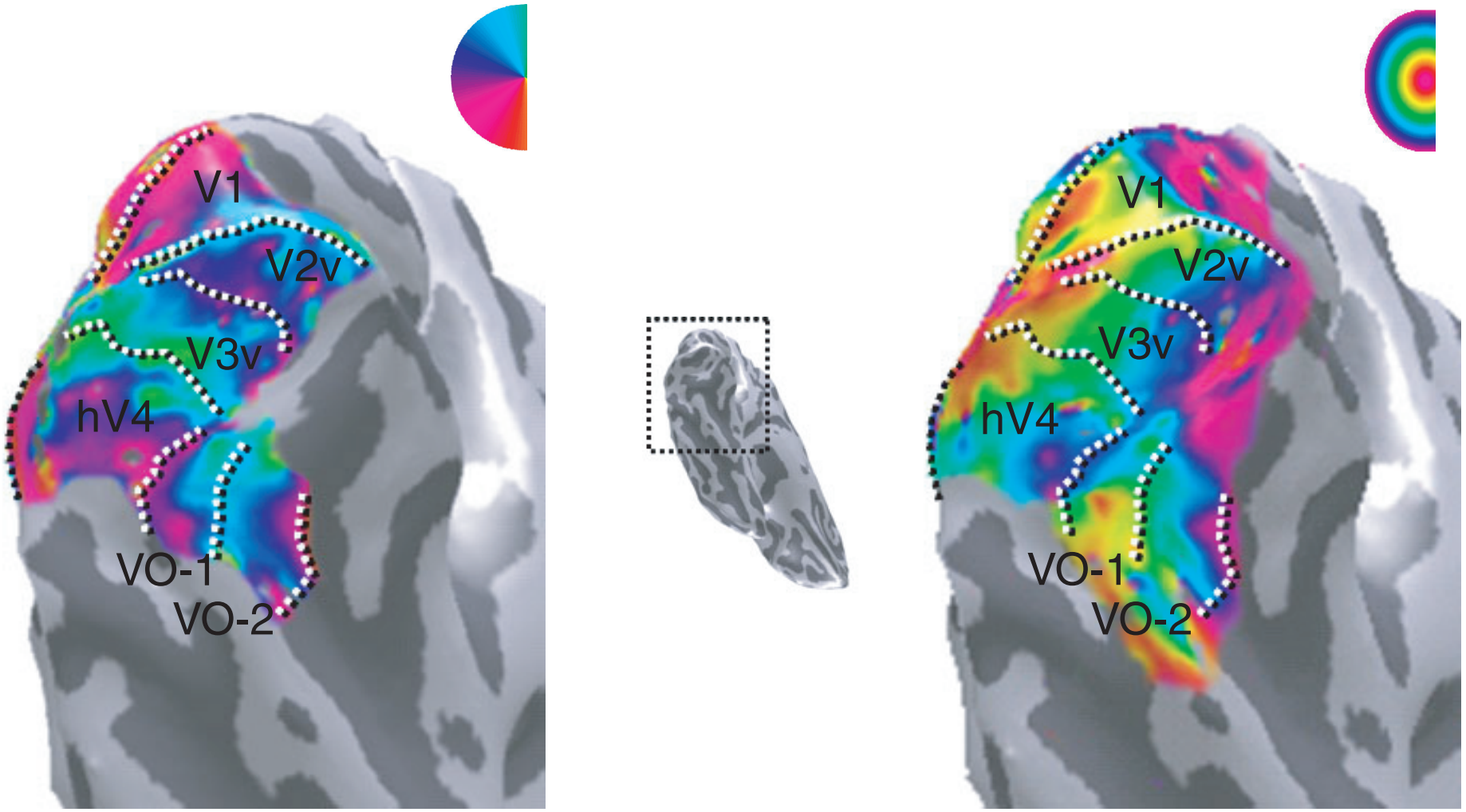

Fig 7

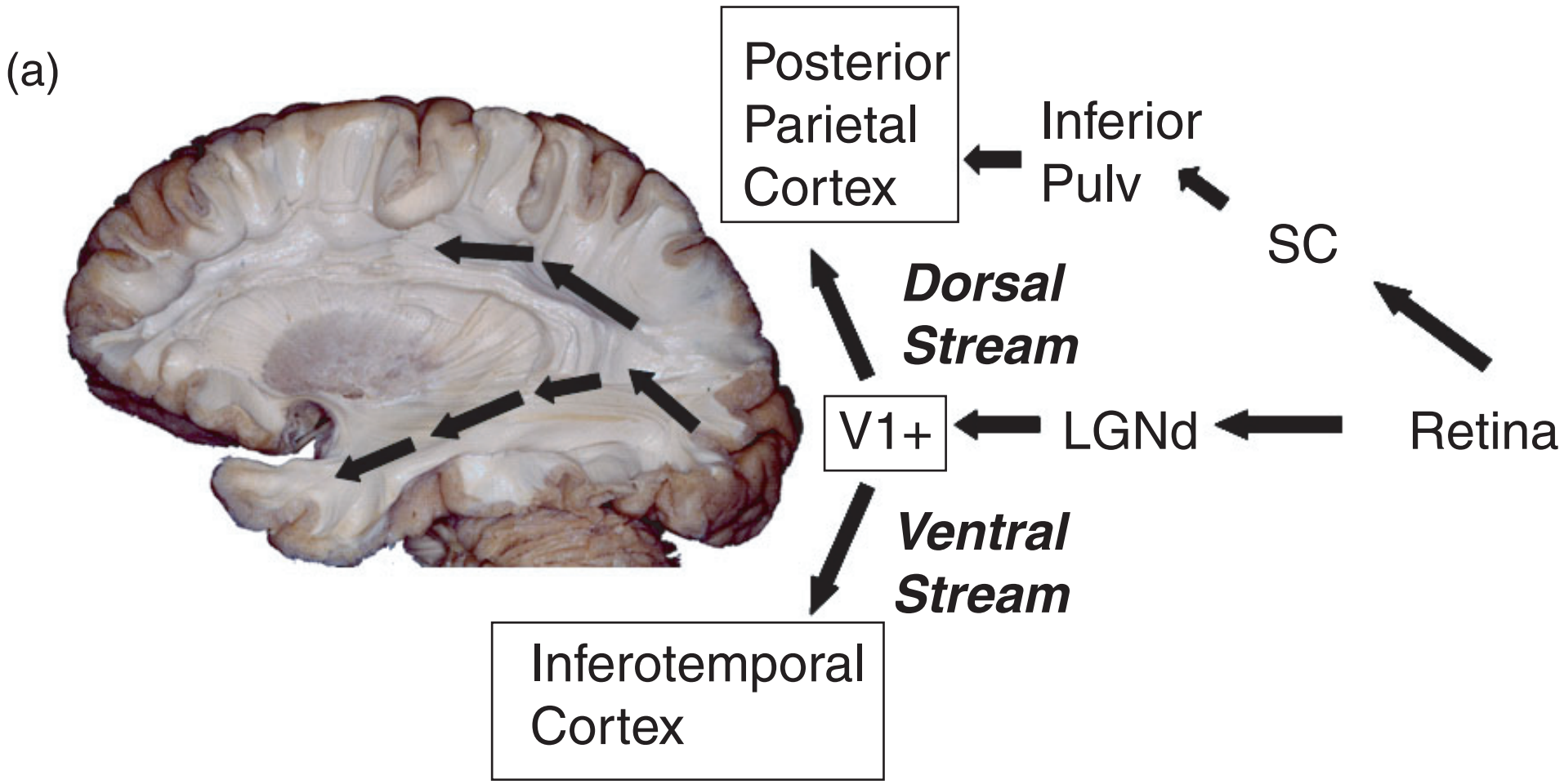
(a)
Posterior Parietal Cortex
Inferior Pulv
SC
Dorsal Stream
V1+
LGNd
Retina
Ventral Stream
Inferotemporal Cortex

Fig 8A

(b)

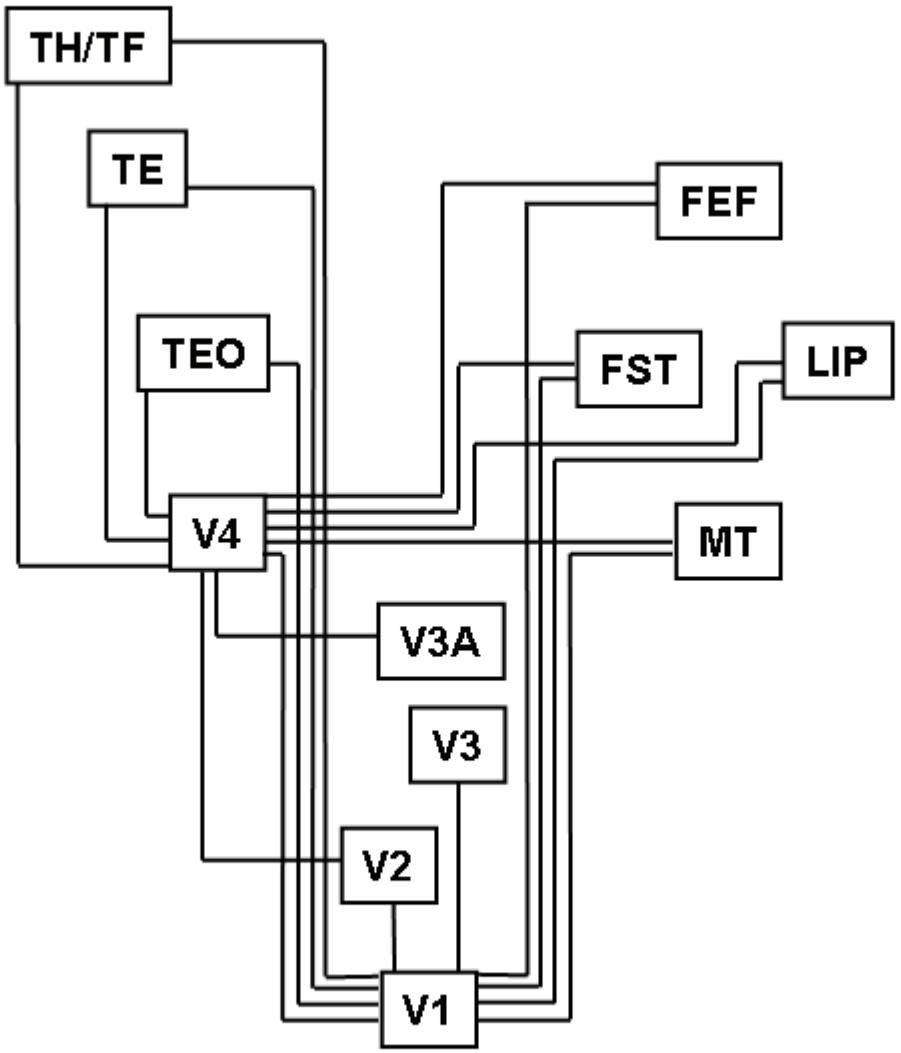

Fig 8B

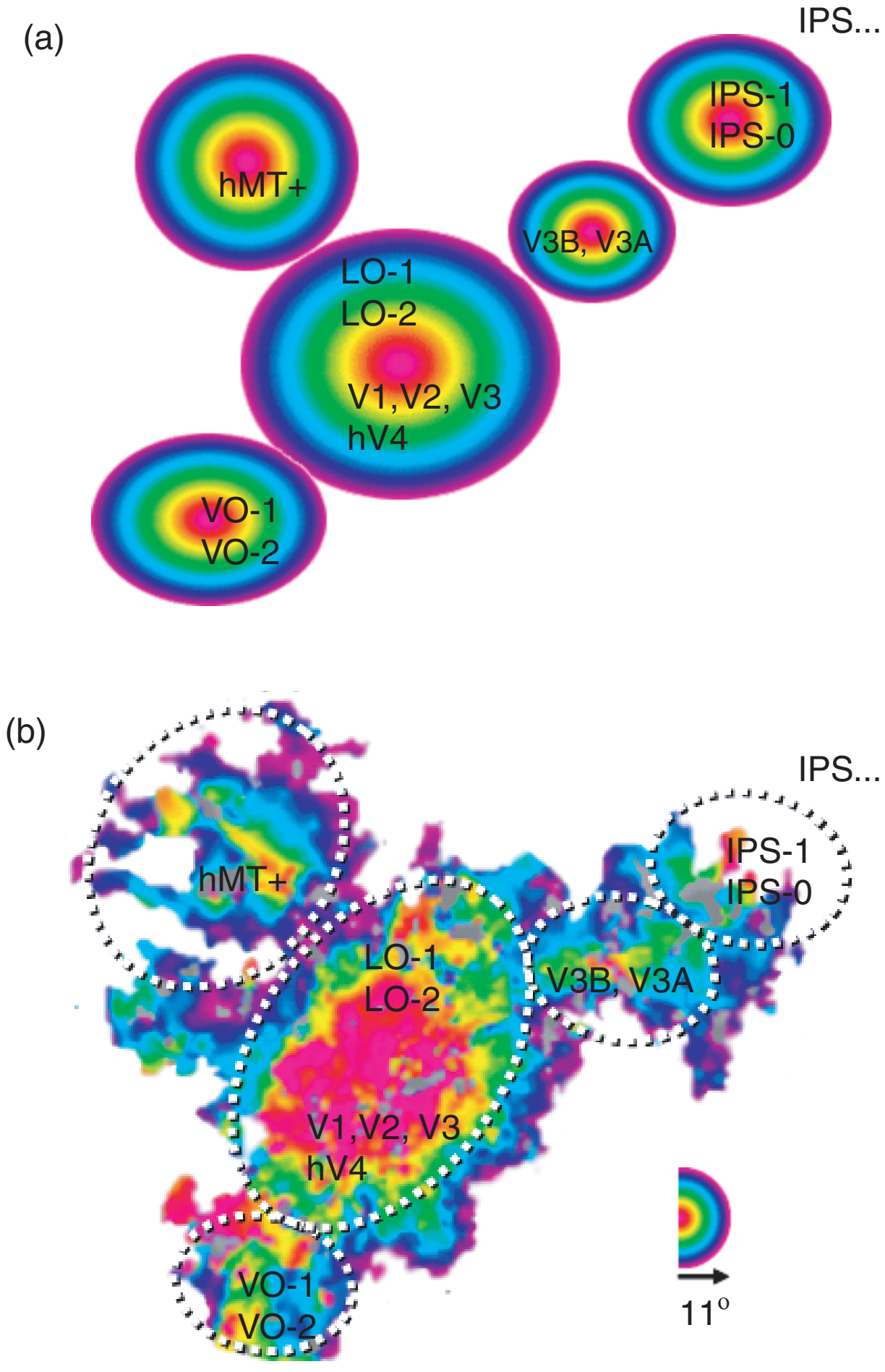
(a)
IPS...
IPS-1
IPS-0
hMT+
V3B, V3A
LO-1
LO-2
V1,V2, V3
hV4
VO-1
VO-2
(b)
IPS...
IPS-1
IPS-0
hMT+
LO-1
LO-2
V3B, V3A
V1,V2, V3
hV4
VO-1
VO-2
11°

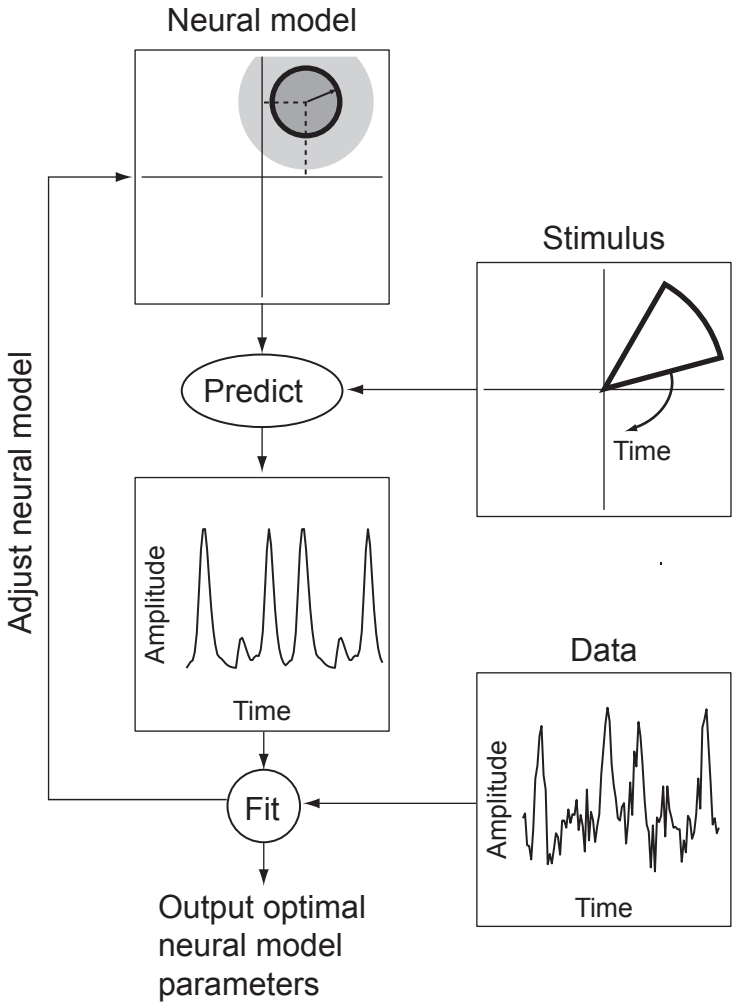
Neural model
Stimulus
Predict
Time
Amplitude
Time
Adjust neural model
Data
Amplitude
Time
Fit
Output optimal
neural model
parameters